Renaissance model of an epidemic with quarantine

Dobay, Akos ; Gall, Gabriella E C ; Rankin, Daniel J ; Bagheri, Homayoun C

Abstract: Quarantine is one possible solution to limit the propagation of an emerging infectious disease. Typically, infected individuals are removed from the population by avoiding physical contact with healthy individuals. A key factor for the success of a quarantine strategy is the carrying capacity of the facility. This is often a known parameter, while other parameters such as those defining the population structure are more difficult to assess. Here we develop a model where we explicitly introduce the carrying capacity of the quarantine facility into a susceptible-infected-recovered (SIR) framework. We show how the model can address the propagation and control of contact and sexually transmitted infections. We illustrate this by a case study of the city of Zurich during the 16th century, when it had to face an epidemic of syphilis. After Swiss mercenaries came back from a war in Naples in 1495, the authorities of the city addressed subsequent epidemics by, among others, placing infected members of the population in quarantine. Our results suggest that a modestly sized quarantine facility can successfully prevent or reduce an epidemic. However, false detection can present a real impediment for this solution. Indiscriminate quarantine of individuals can lead to the overfilling of the facility, and prevent the intake of infected individuals. This results in the failure of the quarantine policy. Hence, improving the rate of true over false detection becomes the key factor for quarantine strategies. Moreover, in the case of sexually transmitted infections, asymmetries in the male to female ratio, and the force of infection pertaining to each sex and class of sexual encounter can alter the effectiveness of quarantine measures. For example, a heterosexually transmitted disease that mainly affects one sex is harder to control in a population with more individuals of the opposite sex. Hence an imbalance in the sex ratios as seen in situations such as mining colonies, or populations at war, can present impediments for the success of quarantine policies.

DOI: https://doi.org/10.1016/j.jtbi.2012.10.002

Renaissance model of an epidemic with quarantine

Akos Dobay[1], Gabriella E. C. Gall [1], Daniel J. Rankin[1], Homayoun C. Bagheri [1]

[1]Institute of Evolutionary Biology and Environmental Studies, Winterthurerstrasse 190, University of Zurich, CH-8057 Zurich, Switzerland

Abstract

Quarantine is one possible solution to limit the propagation of an emerging infectious disease. Typically, infected individuals are removed from the population by avoiding physical contact with healthy individuals. A key factor for the success of a quarantine strategy is the carrying capacity of the facility. This is often a known parameter, while other parameters such as those defining the population structure are more difficult to assess. Here we develop a model where we explicitly introduce the carrying capacity of the quarantine facility into a susceptible-infected-recovered (SIR) framework. We show how the model can address the propagation and control of contact and sexually transmitted infections. We illustrate this by a case study of the city of Zurich during the 16th century, when it had to face an epidemic of syphilis. After Swiss mercenaries came back from a war in Naples in 1495, the authorities of the city addressed subsequent epidemics by, among others, placing infected members of the population in quarantine. Our results suggest that a modestly sized quarantine facility can successfully prevent or reduce an epidemic. However, false detection can present a real impediment for this solution. Indiscriminate quarantine of individuals can lead to the overfilling of the facility, and prevent the intake of infected individuals. This leads to the failure of the quarantine policy. Hence, improving the rate of true over false detection becomes the key factor for quarantine strategies. Moreover, in the case of sexually transmitted infections, asymmetries in the male to female ratio, and the force of infection pertaining to each sex and class of sexual encounter can alter the effectiveness of quarantine measures. For example, a heterosexually transmitted disease that mainly affects one sex is harder to control in a population with more individuals of the opposite sex. Hence an unbalance in the sex ratios as seen in situations such as mining colonies, or populations at war, can present impediments for the success of quarantine policies.

Keywords: epidemic, quarantine, SIR model, reproduction rate, syphilis, modeling infectious diseases

1. Introduction

Although syphilis can be effectively treated with the use of antibiotics since the 1940s, the disease still remains a public health problem worldwide [1, 2]. For instance, the social and economic changes that took place in China in the 1980s were followed by an increase of syphilis cases of about 30% per year by the late 1990s [2]. The rate of infections in Europe have also risen in the last decade [3]. In the 16th century, the city of Zurich faced an epidemic of syphilis [4]. It started when Swiss mercenaries, among them several ill with syphilis, came back from a war in Naples in 1495. At first, the city council tried to contain the epidemic by preventing outside access to the city, and by advising sick people to stay at home and avoid promiscuous public places like churches or markets. Moreover, sex workers were sent away from the city. Later, those who were diagnosed with syphilis, or with similar symptoms, were brought by order of the authorities into a specialized facility. The facility was run by nuns and called the *Blatternhaus*: a word derived from the German *Böse Blattern* (evil pox), which was the description for syphilis at the time. Individuals placed in the *Blatternhaus* were benefiting from special treatments developed for curing people diagnosed with syphilis, or syphilis-like symptoms. Beside the medication itself, the treatment included regular meals with meat and beverage, shelter against the weather, and regular examinations by doctors. Quarantine strategies have been investigated in the past, as isolation remains a potentially effective means to prevent epidemics [5, 6, 7, 8, 9, 10]. For instance, in a study based on the phenomenon of recurrent outbreaks of childhood diseases [6], the authors have shown how isolation can lead to a stable endemic equilibrium for small isolation periods. However, when the size of a population is larger than its census size, which is the case of cities with many visitors, it has been proposed that quarantine can increase the transmission of the disease by increasing the concentration of infected individuals [9].

Previous studies have not explored the effectiveness of quarantine strategies in relation to the carrying capacity of the facility. Here we cover this aspect by showing how the effectiveness of quarantine may depend on this factor. We also wish to understand the potential effectiveness of the decision by the authorities in Zurich to quarantine infected individuals inside the *Blatternhaus*. The answer to these questions can shape future quarantine policies.

In order to quantitatively evaluate the efficiency of quarantine, we developed a model that incorporates the *Blatternhaus* as quarantine facility, and where the rate at which individuals are quarantined is proportional to the amount of spare room inside the quarantine facility. We used the classical SIR approach [11] and extended it with two new states that correspond to individuals isolated from the population. One state or compartment

contains susceptible individuals and the second state, infected ones. We ask whether our model supports the decision of the city council towards reducing or stopping the epidemic.

For our analysis of Zurich during the 16th century, we estimated the size of the population to be 4'000 individuals. Based on the 17th century sketches of the buildings, we also estimated the upper bound of the carrying capacity of the *Blatternhaus* as 100 individuals. Syphilis is caused by both venereal and non-venereal contacts. Instead of starting directly with a sexually transmitted disease (STD), we first considered a contact disease (CD) model. By doing so, we were interested to assess the question whether the same legislation can be efficiently implemented in the case of a CD. The STD model appears then as a direct extension of the CD model by taking genders into account. We show that in both the CD and STD models, the presence of a quarantine facility in the form of the *Blatternhaus* can efficiently reduce or even stop the epidemic, but the effectiveness of quarantine is dependent on the carrying capacity of the *Blatternhaus*, the force of infection, the removal rate, and the effective quarantine rates. We show that without having sophisticated treatment methods nor a complete knowledge of the etiology of the disease, the authorities of the city of Zurich were in the position to find effective measures to reduce the epidemic.

2. Contact disease with quarantine

2.1. Description of the model

One of the earliest epidemic models is that of Kermack and McKendrick [11]. The model in its simplest form assumes the existence of three individual states that are translated into a compartmental approach: susceptible (S), infected (I) and recovered or removed (R). Susceptible and infected individuals are in contact within a homogeneous population. The force of infection is the rate at which susceptible individuals become infected. In our case, the force of infection is a combination of the probability of encounter per capita between susceptible and infected individuals, and the probability to transmit the infection. The rate of recovery defines the time after which the person is not infectious anymore. The SIR approach is characterized by two key parameters: ρ, sometimes called the *relative removal rate*, and R_0, the *basic reproduction rate* [12, 13, 14]. The value R_0, which is also the reciprocal of the relative removal rate ρ, indicates the number of secondary infections produced by one primary infection in an entire population of susceptible individuals. Given a per capita force of infection k_1 and a recovery rate k_2, meaning that the infectious period is $1/k_2$, then $R_0 = k_1 S_0/k_2$, where S_0 is the entire population of susceptible individuals at the time $t = 0$: the moment when a single infected individual is introduced. If $R_0 > 1$ an epidemic will ensue, while if $R_0 \leqslant 1$ the disease will die out and no epidemic will occur since on average every infected person will at most replace itself [15, 16, 17].

Here, the CD model is extended by adding two quarantine states to the standard SIR approach: susceptible (S_B) and infected (I_B) individuals. The subscript B stands for *Blatternhaus*. Figure 1 shows the flow diagram of our CD model with all the five states: S, S_B, I, I_B, and R. The relative rates and their direction are indicated by arrows. The dashed-line arrows display the potential interaction between susceptible and infected individuals. For S_B and I_B, we take into account the possibility to have a reverse rate for individuals excluded from the quarantine facility.

Only primary and secondary syphilis are considered contagious [18, 19]. Transmission is usually by sexual contact, but it may occur by skin contact as well. Subsequently, the disease enters in a latent phase that can last for several years and may remain latent permanently if no treatment is undertaken [19]. Hence, individuals infected by syphilis in the past usually experience symptomatic and not full recovery. Therefore, in our model, R cannot stand reasonably for individuals who recovered, but rather for individuals who are removed, either because they succumb to the disease or because they are not contagious any more, or more probably because they do not show any clinical symptoms.

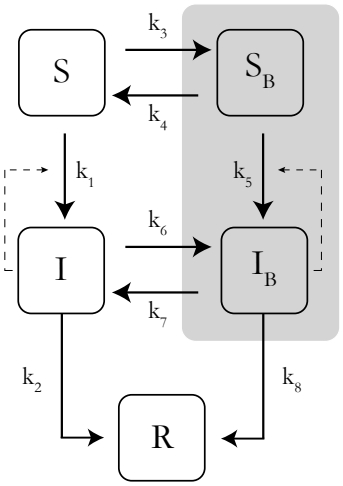

Figure 1: Flow diagram of the SIR-based contact model showing the two classes of individuals in quarantine: S_B and I_B. The parameters k_3 and k_6 in the model are the rates at which individuals are quarantined. The model assumes that the effective rates of quarantine depend on the carrying capacity C of the *Blatternhaus*, which is proportional to $C - S_B - I_B$. At the same time, individuals can be excluded from the quarantine facility, and sent back at a given rate (which is here k_4 and k_7) into the population without recovery, independently from the effective rates of quarantine. For k_3, k_4, k_5, k_6 and k_7 equal to zero, the model reverts to a basic SIR approach.

Furthermore, we assume that the *Blatternhaus* has a carrying capacity C, and the maximum is reached for $S_B + I_B = C$. Under these assumptions, our model is expressed as

$$\begin{aligned}
\frac{dS}{dt} &= -k_1 S I - \kappa_{CD} k_3 S + k_4 S_B \\
\frac{dS_B}{dt} &= -k_5 S_B I_B + \kappa_{CD} k_3 S - k_4 S_B \\
\frac{dI}{dt} &= k_1 S I - k_2 I - \kappa_{CD} k_6 I + k_7 I_B \\
\frac{dI_B}{dt} &= k_5 S_B I_B + \kappa_{CD} k_6 I - k_7 I_B - k_8 I_B \\
\frac{dR}{dt} &= k_2 I + k_8 I_B
\end{aligned} \tag{1}$$

where k_1 is the force of infection, k_2 the recovery rate, and κ_{CD} is defined as

$$\kappa_{CD} = C - S_B - I_B.$$

The parameters k_3 and k_6 present in the model are the quarantine rates, while k_8 is the recovery or removal rate after quarantine. The last two remaining parameters k_4 and k_7 correspond to the rate at which individuals are removed from quarantine before any recovery. The model implies that the effective quarantine rates are proportional to the amount of spare room inside the *Blatternhaus*. This condition is contained in the terms $\kappa_{CD}k_3$ and $\kappa_{CD}k_6$. The choice of setting the effective quarantine rates proportional to the amount of spare room inside the quarantine facility is not the only solution. Another choice could have been to set the effective quarantine rates to a constant value, and quarantine individuals as long as there is spare room inside the quarantine facility. To illustrate this variant, a solution for the case with no false positives can be found in Supplementary Information.

The carrying capacity limits the total number of individuals present inside the *Blatternhaus*, what we express by $0 \leqslant S_B + I_B \leqslant C$. Finally, since we are interested to study the epidemic over a short timescale, we can assume that the population size stays constant, and $S + S_B + I + I_B + R = N$.

In the special case when

$$S(0) = S_0 > 0, I(0) = I_0 > 0, R(0) = 0$$

and

$$S_B(0) = S_{B,0} = 0, I_B(0) = I_{B,0} = 0,$$

one can easily derive an expression for the relative removal rate ρ, and another one for the basic reproduction rate R_0. To do so, we need to solve dI/dt for $t = 0$:

$$\frac{dI}{dt}|_{t=0} = I_0\,(k_1 S_0 - k_2 - k_6 C)\,, \quad \begin{cases} > 0 \\ < 0 \end{cases} \qquad \text{if} \quad S_0 \begin{cases} > \rho(C) \\ < \rho(C) \end{cases}$$

thus the *relative removal rate* becomes

$$\rho = \frac{k_2 + k_6 C}{k_1}. \tag{2}$$

The derivation that corresponds to the general situation where the *Blatternhaus* is not empty at the start (either $I_B(0) \geqslant 0$ or $S_B(0) \geqslant 0$, or both) can be found in Supplementary Information (Equation 1).

The reproduction rate R_0, can be derived from the the relative removal rate since an epidemic starts when

$$S_0 > \frac{k_2 + k_6 C}{k_1}.$$

It follows that

$$R_0 = \frac{S_0 k_1}{k_2 + k_6 C}. \tag{3}$$

Again, the derivation for the general situation where the *Blatternhaus* is not empty at the start is in Supplementary Information (Equation 2). Note that in the numerical analysis of our study, we refer to $R_{0,C=0}$ as the reproduction rate $R_0 = k_1 S_0/k_2$. By this means, one can assess the initial propagation of the disease against the carrying capacity of the *Blatternhaus*. Equation 3 indicates that a higher C would decrease R_0.

2.2. *Numerical analysis with no false detection ($k_3 = 0$ and $S_B = 0$)*

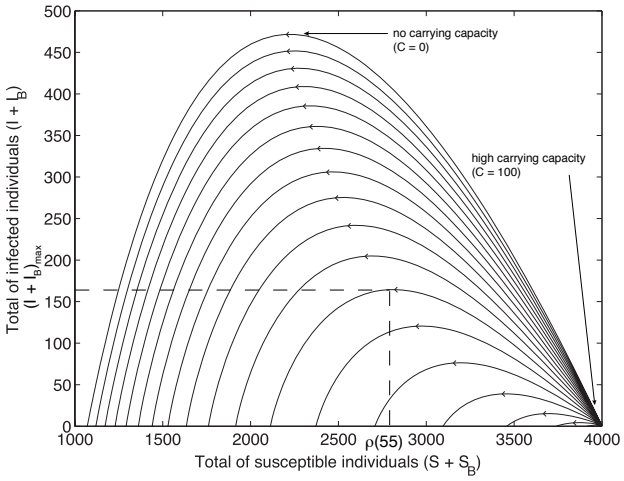

Figure 2: Phase trajectories in the susceptible versus total infected individuals plane with no false detection ($k_3 = 0$ and $S_B = 0$). All the trajectories are determined by the same force of infection $k_1 = 5 \cdot 10^{-6}$. The different trajectories correspond to different values of the carrying capacity C, ranging from 0 (no carrying capacity or no *Blatternhaus*) to 100. Given our initial number of susceptible individuals, this force of infection is equivalent to a basic reproduction rate (without quarantine facility) of $R_0 = 2$. The plots are determined by the initial conditions $S(0) = 3999$, $S_B(0) = 0$, $I(0) = 1$, $I_B(0) = 0$ and $R(0) = 0$. The remaining parameters in the model are: the population size $N = 4'000$, $k_2 = 1/90$, $k_4 = 0$, $k_5 = 0$, $k_6 = 1 \cdot 10^{-4}$, $k_7 = 1 \cdot 10^{-5}$, $k_8 = 1/70$. The relative removal rate $\rho(55)$ for the trajectory corresponding to a carrying capacity of 55 individuals has been highlighted. If $S(0) < \rho(55)$, in the case where the *Blatternhaus* can welcome up to 55 patients, no epidemic will occur, and the disease will die out. The value of ρ can be computed by taking the general relation derived in Appendix A.1, and replacing $I_{B,0}$ by its actual value, which is here approximately 28. The calculation gives $\rho(55) = (k_2 + k_6(C - I_{B,0}) - k_7 I_{B,0})/k_1 = (1/90 + 1 \cdot 10^{-4}(55 - 28) - 28 \cdot 10^{-5})/5 \cdot 10^{-6} = 2706$. In comparison to the classical SIR phase plane, here all the trajectories correspond to the same S_0 and I_0, and all the curves are starting at the bottom left of the plane.

Using numerical routines in *Matlab*, we analyzed the present model. First, we looked into the literature to obtain an estimate of the reproduction rate for syphilis. A value of $R_0 = 1.15$ was given in [20]. To cover a wider scenario, we took an interval ranging from 1 to 2. Based on our initial number of susceptible individuals, this corresponds to a value of k_1 between $2.5 \cdot 10^{-6}$ and $5 \cdot 10^{-6}$. We also looked into the literature to obtain an estimate of the recovery period. The recovery period can be very variable. Usually the chancre of the primary stage lasts 3 to 6 weeks, and can heal without treatment [18]. The incubation time can range from 1 to 13 weeks [19]. The symptoms of the secondary stage typically begin 6 to 12 weeks after the chancre has appeared [19]. Altogether, the symptoms of the first two stages may last between 6 to 15 weeks [19]. It is probably the case that infected individuals exhibiting healing lesions were asked to leave the *Blatternhaus*. We set the recovery period to 90 days outside, and 70 days inside the *Blatternhaus*.

The choice of a shorter recovery period inside the *Blatternhaus* is based on the assumption of special cares given for patients. This period correlates with the moment when the symptoms of the first and the second stages are visible.

We also addressed the quarantine rates k_3 and k_6. Intuitively, the rate of quarantine depends on the size of the population N, the efficiency of the detection method, and the recovery rate k_2. Infected individuals in a large population are more difficult to locate, and a short recovery period may prevent the person to be detected on time. There still might be other factors which cannot be quantified, for instance policies for infected individuals, that can influence k_3 and k_6. However, it is possible to express the quarantine rates k_3 and k_6 as

$$k_3 = \frac{d_s}{Nk_2},$$

and

$$k_6 = \frac{d_i}{Nk_2},$$

where $d_\bullet$ is the apparent detection rate, and will have different values for susceptible (d_s: false detection) and infected individuals (d_i: true detection). There is of course no standard definition for how to set d_s and d_i, but we infer that increasing the value of d_i will improve the effective detection of infected individuals, while decreasing the value of d_s will similarly improve the effectiveness of the quarantine. Using this definition and a corresponding value for k_6 of $1 \cdot 10^{-4}$ (since $k_3 = 0$), which uses an effective detection value of $d_i = 4/9 \cdot 10^{-2}$, it is sufficient to stop the epidemic with a carrying capacity between 80 to 100, even in the case of a reproduction rate R_0 of 2 (see for instance Figure 3).

Regarding k_7, it is difficult to quantify the exclusion rate from the *Blatternhaus*. Exclusions are probably based on internal policies and vary from case to case. For our analysis, we choose k_7 to be 10 times smaller than k_6.

In Figure 2 we show the susceptible-infected phase plane in the case when, at the start, the *Blatternhaus* is empty ($S_B(0) = 0, I_B(0) = 0$), and there is one infected individuals in the entire population. Each trajectory in the phase plane is defined by the same initial conditions ($S(0) = 3999, I(0) = 1, R(0) = 0$), and corresponds to the progression of the epidemic for different values of the carrying capacity C. As we can see, with increasing carrying capacity, the maximum of the total number of infected individuals ($(I + I_B)_{max}$) decreases. Note that in comparison to the classical SIR epidemic phase plane, the trajectories in Figure 2 have all the same starting conditions, while in the representation of the classical SIR system each trajectory has a different set of initial conditions.

Figure 3A plots the maximum of the total number of infected individuals ($I + I_B$), while Figure 3B displays the total number of removed individuals R, both against the force of infection and the carrying capacity. The maximum size of the epidemic with no quarantine is given by the value of R_{max} at $C = 0$. This number can serve as a reference value to gauge the impact of the quarantine while increasing C. Furthermore, it is possible to show that k_6 directly controls the size of the epidemic by increasing or decreasing it's value. For instance, a five-fold increase in k_6 will result in a four-fold decrease in the total number of infected people ($I + I_B$). In order to compare the change in dynamics from a weak to a strong force of infection, we plotted the curves of $(I + I_B)_{max}$ and R_{max} for three different values of $R_{0,C=0}$ against the carrying capacity C (Figure 3C and 3D). As we mentioned earlier, we use the convention $R_{0,C=0}$ to allow us to give an idea of how at constant reproductive rate, the disease will spread with increasing carrying capacity. According to our model, the reproductive rate varies with C, and therefore a more appropriate view is given by the phase trajectories.

Another aspect in this model is the distinction between individuals that are removed after having healed or died, and those who leave the *Blatternhaus* and are still infected. To test this situation, we set k_7 and k_8 to the same value. In that case, our estimated carrying capacity would need to be about twice as much as in our current analysis in order to stop an epidemic with a reproductive rate $R_{0,C=0} = 2$.

2.3. Effects of false detection ($k_3 > 0$ and $S_B > 0$)

When we introduce false detections in the model, the progression of the epidemic changes. False detections, or a blind prevention consisting of selecting susceptible individuals to be quarantined, has detrimental consequences on the spread of the disease. If the facility has a finite carrying capacity, the intake of uninfected individuals will prevent infected individuals to be quarantined. When the force of infection is weak there will be a tendency to send more susceptible individuals to the *Blatternhaus* than infected ones. This is apparent when we compare Figures 3C and 4C. At a reproductive rate $R_{0,C=0} = 1.35$, the ratio between the carrying capacity required to stop the epidemic with and without false detections is circa thirty times bigger, while for $R_{0,C=0} = 2$ this ratio is reduced by half.

Conceptually, this model is comparable to a vaccination campaign where healthy individuals are selected to be treated without representing a target group. Since vaccines are available in limited quantities, such strategy can prevent stopping the epidemic [12].

Given false detections, Figures 3C and 4C clearly show that at similar carrying capacities, quarantine can no longer help to stop the epidemic. We also plotted the trajectories of the epidemic in the phase plane (see Figure 5). Again, when false detection occurs and susceptible individuals are in the *Blatternhaus*, the maximum of total infected individuals is raised, even at the highest of the carrying capacity of the *Blatternhaus*.

2.4. Model behavior for larger population size

Finally, we tested our CD model for larger population sizes without false detections. To do so, we increased the population size, and compared the behavior of the model to our original size of 4'000 individuals. At the same time, we adjusted the force of infection, since in our case $k_1 = k_2 R_0 / S_0$. When increasing the population size to 16'000, we observe that the impact of the *Blatternhaus* on the epidemic size is effective only at larger carrying capacities compared to to our original size of 4'000 individuals (see supplementary Figures 2A and 2B).

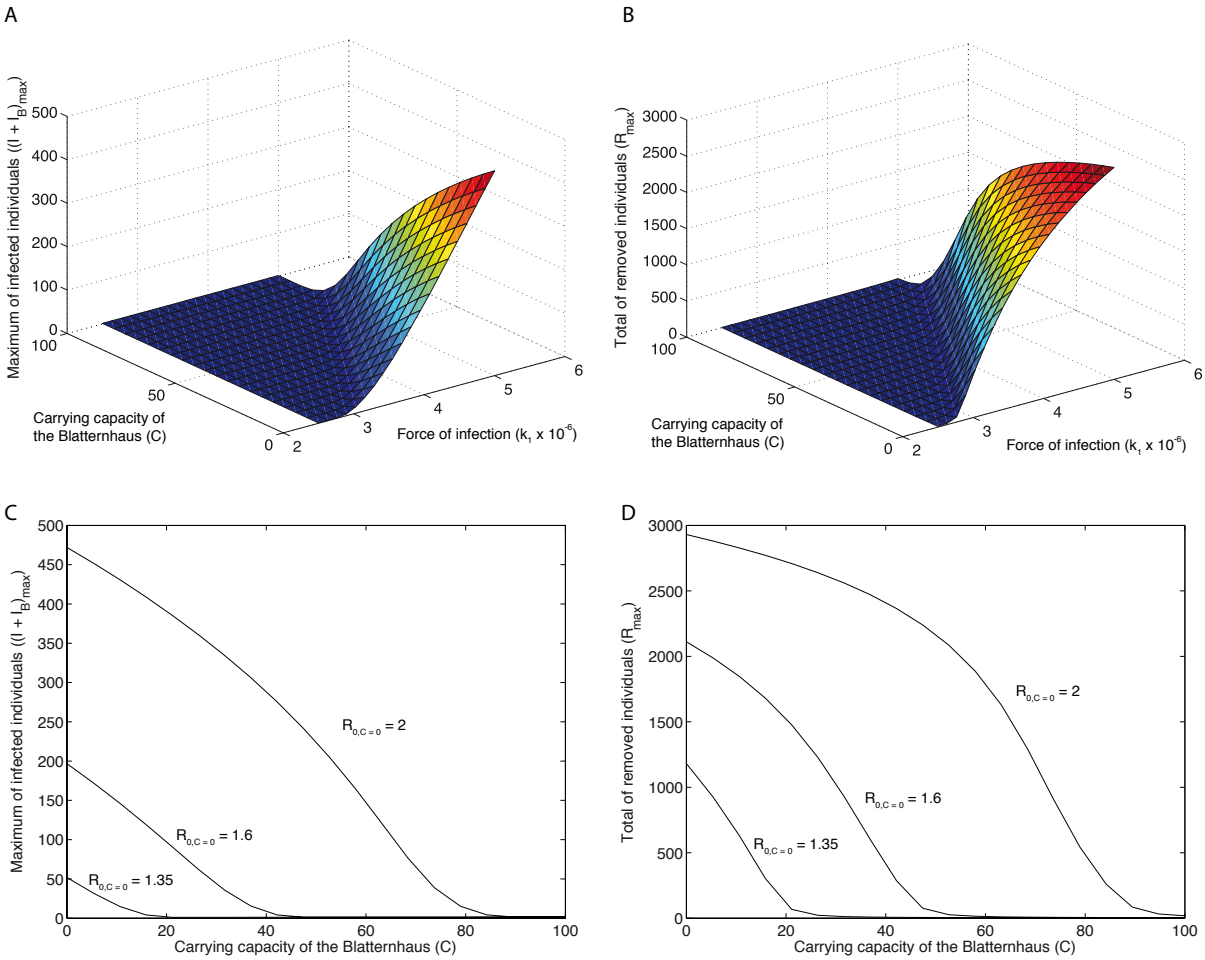

Figure 3: Numerical analysis of the contact model with no false detection ($S_B = 0$ and $k_3 = 0$). This model describes a situation where only infected individuals are quarantined in the *Blatternhaus*. The maximum of the total number of infected individuals inside and outside the *Blatternhaus* $(I + I_B)_{max}$ (A) and the total number of recovered/removed individuals R_{max} (B) at $t(\infty)$ are displayed as function of the carrying capacity C of the *Blatternhaus* and the force of infection k_1. The profile of three distinct reproduction rates $R_{0,C=0} = 1.35$, $R_{0,C=0} = 1.6$ and $R_{0,C=0} = 2$ are visible, showing the relationship between $(I + I_B)_{max}$ (C) and R_{max} (D) and the carrying capacity of the *Blatternhaus*. The remaining parameters in the model, as well as the initial conditions, can be obtained from Figure 2.

The model also exhibits a sharper transition that corresponds to biphasic states where a small increase in the carrying capacity manifests a sudden drop in the maximum of infected individuals (see supplementary Figure 2B). The more we increase the population size, while keeping the quarantine rates identical to our original population size, the sharper the transition between the biphasic states (see supplementary Figures 2C and 2D). In other words, the effectiveness of quarantine becomes more sensitive to the carrying capacity in larger populations.

3. Sexually transmitted disease with quarantine

In the previous section we described an SIR approach with quarantine to analyze the outbreak of syphilis as a contact disease (CD). A sexually transmitted disease (STD) can be considered as a subset of contact models, where transmission occurs as a result of heterosexual and homosexual encounters in the population. In this section, we analyze the outbreak of syphilis as an STD, and compare the results to our CD model.

3.1. Description of the model

The STD model introduces a layer of refinement by discriminating males and females in the population. Figure 6 gives a description of the flow between the different classes of individuals and their corresponding exchange rates. The model follows a criss-cross model of disease in which susceptible males are the host for infected females, and vice versa [12, 21]. For simplicity, we assume that the population exhibits a uniform level of promiscuity, and the probability that a male meets a female, or the other way around, is equal for every male or female in the population respectively. There is no paring or subgroups. However, the model includes homosexual encounters, referred to as MSM (Males having Sex with Males) and FSF (Females having Sex with Females). The male population is divided into susceptible ($S_{\male}$) and infected ($I_{\male}$) individuals. Similarly, the female population is divided into susceptible ($S_{\female}$) and infected ($I_{\female}$) individuals. The model makes no distinction between recovered or removed males or females: both are modeled with the same compartment R. The individuals in the *Blatternhaus* are also following the same type of division into susceptible ($S_{\male B}$) and

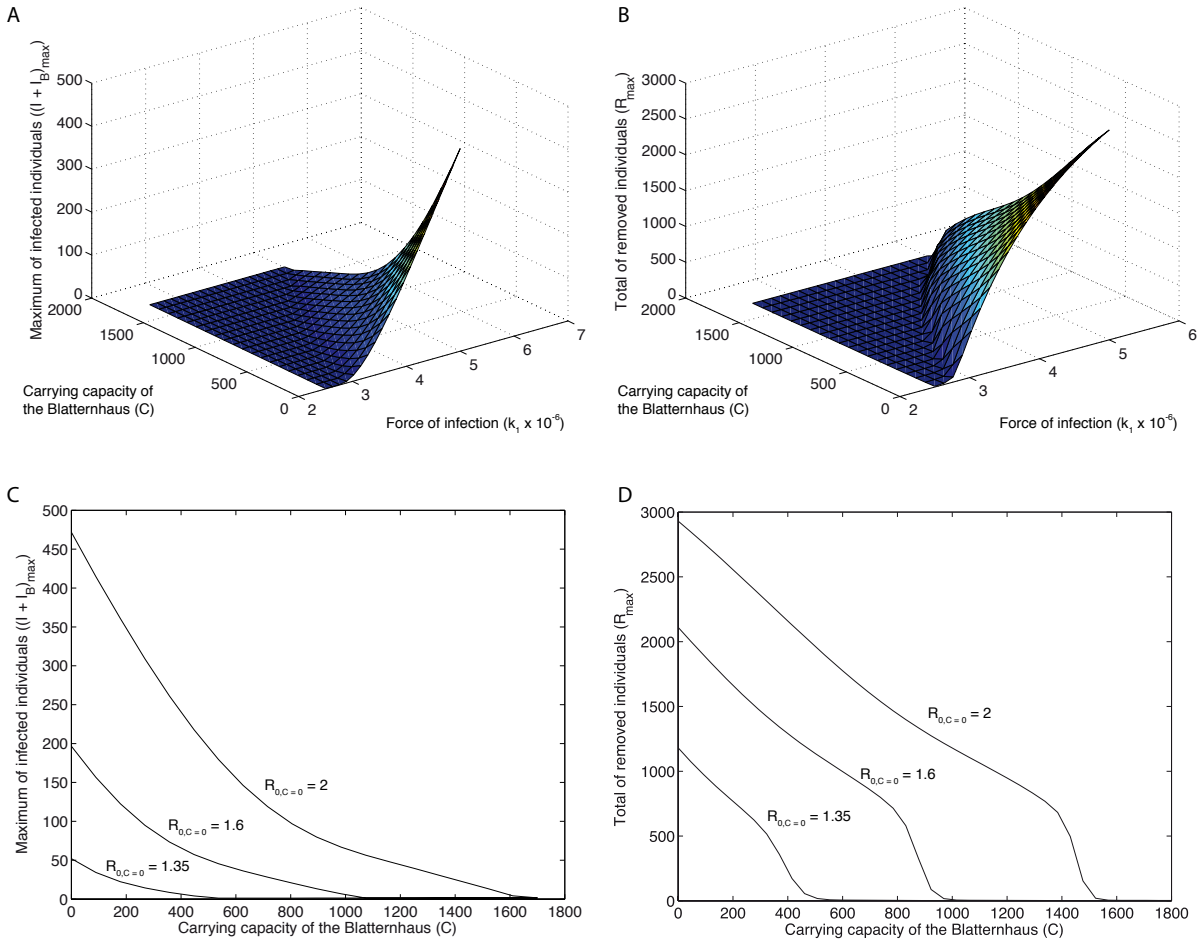

Figure 4: Numerical analysis of the contact model with false detections ($S_B > 0$ and $k_3 = 2 \cdot 10^{-7}$). (A) to (D) correspond to the situation where individuals are not diagnosed properly, or are intentionally isolated from the population to be place in quarantine. These latter individuals are, for instance, more susceptible than the others to become infected. The parameters of the run can be obtained from Figure 2 and 5.

infected ($I_{\male B}$) males, and susceptible ($S_{\female B}$) and infected ($I_{\female B}$) females.

Based on the assumptions we summarized above, our STD model can be expressed using the following set of ordinary differential equations:

$$
\begin{aligned}
\frac{dS_{\female}}{dt} &= -k_1^{\female} S_{\female} I_{\male} - k_1^{\female\male} S_{\female} I_{\female} - \kappa_{STD} k_3^{\female} S_{\female} + k_4^{\female} S_{\female B} \\
\frac{dS_{\male}}{dt} &= -k_1^{\male} S_{\male} I_{\female} - k_1^{\male\male} S_{\male} I_{\male} - \kappa_{STD} k_3^{\male} S_{\male} + k_4^{\male} S_{\male B} \\
\frac{dS_{\female B}}{dt} &= -k_5^{\female} S_{\female B} I_{\male B} - k_5^{\female\female} S_{\female B} I_{\female B} + \kappa_{STD} k_3^{\female} S_{\female} - k_4^{\female} S_{\female B} \\
\frac{dS_{\male B}}{dt} &= -k_5^{\male} S_{\male B} I_{\female B} - k_5^{\male\male} S_{\male B} I_{\male B} + \kappa_{STD} k_3^{\male} S_{\male} \\
&\quad -k_4^{\male} S_{\male B} \\
\frac{dI_{\female}}{dt} &= k_1^{\female} S_{\female} I_{\male} + k_1^{\female\female} S_{\female} I_{\female} - k_2 I_{\female} - \kappa_{STD} k_6^{\female} I_{\female} + k_7^{\female} I_{\female B} \\
\frac{dI_{\male}}{dt} &= k_1^{\male} S_{\male} I_{\female} + k_1^{\male\male} S_{\male} I_{\male} - k_2 I_{\male} - \kappa_{STD} k_6^{\male} I_{\male} \\
&\quad +k_7^{\male} I_{\male B} \\
\frac{dI_{\female B}}{dt} &= k_5^{\female} S_{\female B} I_{\male B} + k_5^{\female\female} S_{\female B} I_{\female B} - k_8 I_{\female B} + \kappa_{STD} k_6^{\female} I_{\female} - k_7^{\female} I_{\female B} \\
\frac{dI_{\male B}}{dt} &= k_5^{\male} S_{\male B} I_{\female B} + k_5^{\male\male} S_{\male B} I_{\male B} - k_8 I_{\male B} + \kappa_{STD} k_6^{\male} I_{\male} \\
&\quad -k_7^{\male} I_{\male B} \\
\frac{dR}{dt} &= k_2 (I_{\female} + I_{\male}) + k_8 (I_{\female B} + I_{\male B})
\end{aligned}
\tag{4}
$$

where κ_{STD} is defined as

$$\kappa_{STD} = C - S_{\female B} - S_{\male B} - I_{\female B} - I_{\male B}.$$

The other parameters in the model are $k_1^{\male}$ and $k_1^{\female}$, the force of infection for infected males having sex with susceptible females, and vice versa. A similar definition holds for $k_5^{\male}$ and $k_5^{\female}$, the forces of infection inside the *Blatternhaus*. The MSM and FSF encounters have the rates $k_1^{\male\male}$, $k_5^{\male\male}$, $k_1^{\female\female}$, and $k_5^{\female\female}$ respectively. The quarantine rates are $k_3^{\female}$, $k_3^{\male}$, $k_6^{\female}$ and $k_6^{\male}$. The rates of exclusion are $k_4^{\female}$, $k_4^{\male}$, $k_7^{\female}$ and $k_7^{\male}$. The rate of recovery of removal is k_8, which is equal for both genders. As in

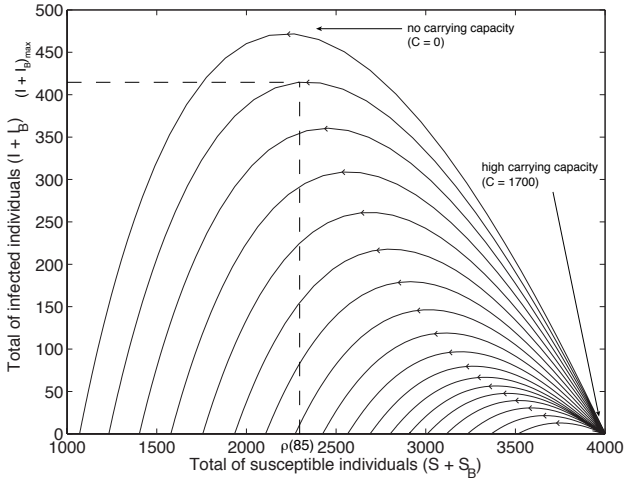

Figure 5: Phase trajectories in the susceptible versus total number of infected individuals plane with false detections ($S_B > 0$ and $k_3 = 2 \cdot 10^{-7}$). All the trajectories are determined by the same force of infection $k_1 = 5 \cdot 10^{-6}$. The remaining parameters, as well as the initial conditions can be obtained from Figure 2, excepted $k_4 = 2 \cdot 10^{-7}$, $k_5 = 1 \cdot 10^{-7}$, $k_6 = 1 \cdot 10^{-5}$, and $k_7 = 1 \cdot 10^{-6}$. The value of ρ is computed in a similar way as in Figure 2, replacing simultaneously $S_{B,0}$ and $I_{B,0}$ by their actual values, which is here approximately 10 and 43 respectively. The calculation gives $\rho(85) = (k_2 + k_6(C - S_{B,0} - I_{B,0}) - k_7 I_{B,0})/k_1 = (1/90 + 1 \cdot 10^{-5}(85 - 10 - 43) - 43 \cdot 10^{-6})/5 \cdot 10^{-6} = 2277$.

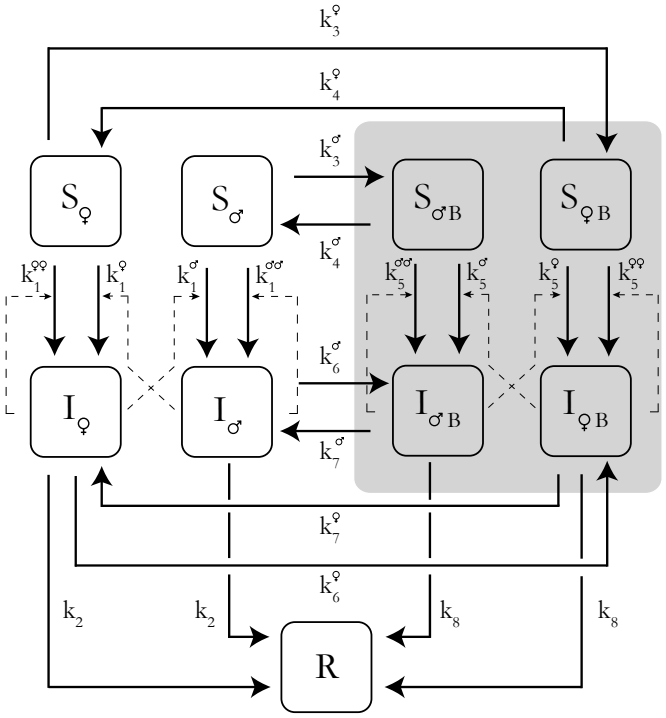

Figure 6: Flow chart of the sexually transmitted disease model with quarantine.

the case of the CD model, we also assume that the population size stays constant over the course of the epidemic, and $S_♀ + S_{♀B} + I_♀ + I_{♀B} = N_♀$ and $S_♂ + S_{♂B} + I_♂ + I_{♂B} = N_♂$.

Note that our STD model is symmetric with respect to all its gender variables, as long as the rates are equal for males and females. Therefore, in the numerical analysis, when the rates are equal for both genders, we will only show the result for one gender.

3.2. *Numerical analysis with no false detection ($k_3^♂ = k_3^♀ = 0$ and $S_{♂B} = S_{♀B} = 0$)*

Using numerical routines in *Matlab*, we analyzed the STD model. Since we previously estimated the total population to 4'000 individuals, we assumed that only half of them are sexually active. We first looked at the change in the maximum of infected males ($(I+I_{♂B})_{max}$) as a result of increasing force of infections ($k_1^♂$), and by taking the rates we used in the CD model and setting them equal for both genders. In the case when males and females are equal in number, and in comparison to the CD model, we observe a relative increase in $(I + I_B)_{max}$ at larger carrying capacity (see Figure 7A and B, and Figure 3). In order to directly compare the size of the epidemic between the two models, we performed an analysis where the sexually active population was increased to 4'000, while keeping the same rates as in the CD model. In that case, there was no significant difference in the resulting dynamics of the epidemic: by adding infected males and females, the maximum of infected individuals is close to 500 (see Figure 7C and D, and Figure 3).

The STD model becomes interesting when the number of males and females differs substantially, or when the force of infection for males and females is different. The former case can for instance occur after a long war, where males are systematically sent away to the front. Other examples are small industrial enclaves such as mining colonies, where males are in the majority. In such cases, the STD model should give a better prediction on the number of infected males and females, and how the quarantine procedure affects the overall dynamics of the disease.

We examined at the case where the force of infection for females is four times larger than the one for males. When the carrying capacity is small, the difference in the force of infection will be reflected in the total number of infected males and females. By increasing the carrying capacity of the *Blatternhaus*, it is possible to reduce the difference in the number of infected males and females until almost no difference is observed (see supplementary Figure 3). We also looked at the situation where the number of males and females differs substantially. To investigate this situation, we set the number of males to 500 and the females to 1500, but we kept the rates equal for both sexes. Again, when the carrying capacity is small, the difference in the number of infected males and females is significant (see supplementary Figure 4).

Finally, we tested the effect of adding homosexual intercourses. We set the forces of infection $k_1^{♀♀}$ and $k_1^{♂♂}$ to $1 \cdot 10^{-5}$ and $5 \cdot 10^{-6}$ respectively. Homosexual intercourses affect the overall dynamics of the epidemic. The presence of MSM and/or FSF type of individuals increases not only the maximum number of infected individuals, but in order to stop the epidemic, one needs to increase the carrying capacity of the *Blatternhaus* (see supplementary Figure 5). This effect can be explained if

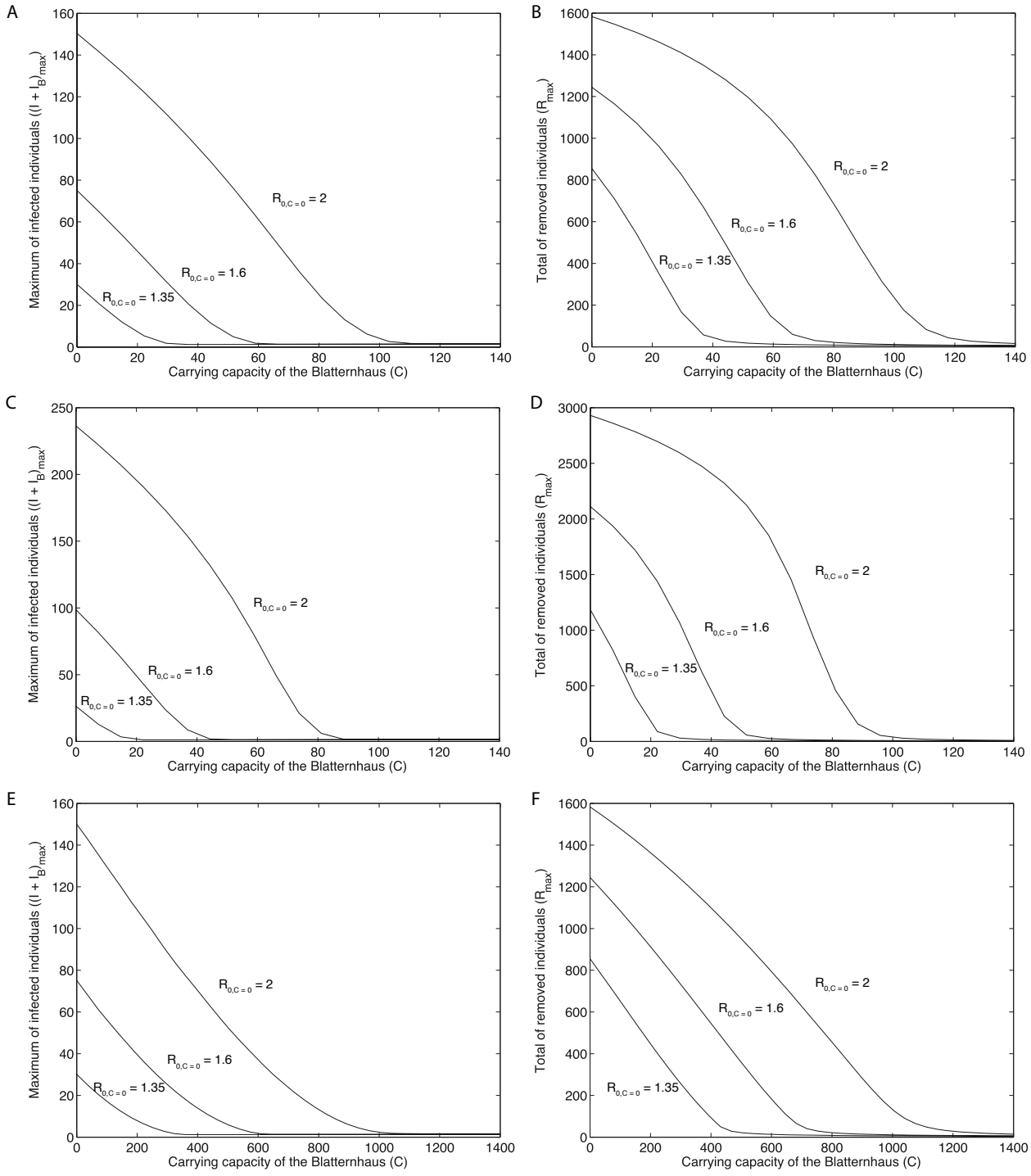

Figure 7: Numerical analysis of the STD model. (A) to (D) were obtained with no false detection. In (A) and (B) the population size is 2'000, with an equal number of males and females, while in (C) and (D) we increased the population size to 4'000 in order to compare the STD model with the CD model. In panels (E) and (F) the population size is 2'000 with false detections. The other parameters of the runs can be obtained from Figure 2 and 4.

we consider the fact that adding homosexual intercourses partly reverts the STD model into a CD model by allowing the transmission of the disease between individuals of the same sex. Indeed, in the case where the rates for males and females in all encounters are equal, it is possible to show that the STD model algebraically reduces to the CD model (see section C in the Supplementary Information). However, if the rates for males and females are different, the two models have different expressions. In such a case, the correct way to take into account the presence of MSM and/or FSF type of individuals is by adjust-

ing the force of infection for each type of individuals such that it properly reflects the fraction of homosexual and heterosexual intercourses in the population. Note that our model does not make a sharp distinction between homosexual and heterosexual individuals, and describes a situation where individuals can be involved in both homosexual and heterosexual intercourses.

Figure 8 shows how the final epidemic size R_{max} depends on the ratio between males and females, and the presence or absence of MSM and FSF individuals. This result is obtained by systematically varying the number of females from 0 to 2'000, while keeping the sum of males and females constant. The top of the vertical axis in each panel corresponds to the situation where there is no males, and only females are present in the population. Similarly, at the bottom of the vertical axis, there is only males in the population. By moving away from these two extremes towards the center of the vertical axis, we increase the number of susceptible individuals of the opposite sex. Since $dI_{\male}/dt$ is proportional to $S_{\male}$, and $dI_{\female}/dt$ to $S_{\female}$ respectively, we also increase subsequently the number of infected individuals of the opposite sex. Hence, R_{max} increases as we approach the midpoint of the vertical axis. In order to reduce the size of the epidemic, one has to either increase the carrying capacity of the *Blatternhaus* by moving along the horizontal axis, or increase the asymmetry between males and females by moving along the vertical axis. In a strictly homosexual population, the situation changes, and the asymmetry between males and females increases the number of infected individuals (Figure 8D). As long as we deal with a well-mixed population of males and females (indicated by the dashed-line) there is no substantial difference in the epidemic size between a heterosexual and a homosexual population.

Another aspect in Figure 8 is the rate at which R_{max} changes. This information is contained in the distance between the R_{max} isolines. As the distance between isolines gets smaller, the force of infection changes more rapidly.

The contour maps showed in Figure 8 can also teach us about the different epidemic scenarios we can encounter for STDs. In a strictly heterosexual population, the epidemic will always do better in a balanced male:female ratio (see Figure 8A and supplementary Figure 6A), while in a population dominated by homosexual encounters it is harder to stop an epidemic when moving away from a 1:1 ratio (see Figure 8D). The dynamics changes if the rates are different for males and females. If males are more susceptible, and the pathogen is carried by female individuals, then R_{max} is higher if the population has more females (see Figure 8B). Adding MSM encounters will amplify the phenomenon (see Figure 8C). If there is further heterogeneity in the force of infection for different classes of sexual encounters, one obtains further asymmetries in R_{max} isoclines (see supplementary Figure 6B).

3.3. Effects of false detection ($k_3^{\male}, k_3^{\female} > 0$ and $S_{\male B}, S_{\female B} > 0$)

As in the case of the CD model, adding false detections has detrimental consequences on controlling the spread of the disease. Using the same rates as in the CD model with false detections, and a reproductive rate $R_{0,C=0} = 2$ in a population of 2'000 individuals, false detections in the STD model shift the carrying capacity required for stopping the epidemic from 100 to 1200. This number represents 70% of the population size. A slightly higher amount compared to the CD model, where false detections lead to almost 50% (42%) of the population size as carrying capacity of the *Blatternhaus* to stop the epidemic. Our analysis shows how easily false detections can defeat the purpose of having a quarantine facility in both the CD and STD cases. If a quarantine facility with a large carrying capacity is misused by having a bad detection rate, then the epidemic will mainly occur outside the facility (see supplementary Figure 7). Even if the rate of true detection is further improved, the quarantine facility may well contain the first wave of epidemic, but the constant intake of uninfected individuals inside the quarantine facility will fail to control the second wave when the number of infected individuals has reached a given threshold to initiate a new epidemic (see supplementary Figure 7B).

3.4. Importance of the ratio of true to false detections

In sections 2.3 and 3.3 we analyzed the effects of false detection on the spread of the disease. We showed that false positives diminish the effectiveness of quarantine. Since the rates of true and false detections are independent of each other we examined combinations of k_6 to k_3 to assess effectiveness of quarantine strategies. For each carrying capacity between 0 and 1600 we searched for the ratios that can prevent an epidemic. We define C_0 as the carrying capacity at which R_{max} is at most less than 0.1% of the total population. The same definition naturally holds for other threshold values. Figure 9 summarizes the effectiveness of the quarantine strategy by showing the carrying capacity at a given ratio of k_6 over k_3 required to prevent an epidemic for both CD and STD. The data points were obtained by systematically varying the quarantine rates k_3 and k_6 from $2 \cdot 10^{-10}$ to $1.4 \cdot 10^{-6}$ and $1 \cdot 10^{-8}$ to $4 \cdot 10^{-4}$ respectively. For each combination of k_6 over k_3, the maximum value of R_{max} is stored until it drops the first time below 0.1% of the total population.

As we can see in Figure 9, in order to prevent an epidemic using a small carrying capacity, one needs a high k_6 to k_3 ratio.

4. Discussion

Using both CD and STD models, we evaluated the situation of a 16$^{\text{th}}$ century European city, and its policy in preventing an epidemic of syphilis. Our results suggest that the decision of the authorities to systematically quarantine infected individuals, and keep them under medical control while providing the necessary care to heal them, can help to stop the epidemic. Such legislation is probably more effective than simply advising sick people to stay at home and avoid public places, and can justify the motivations of the city council to institute the *Blatternhaus*.

Even if syphilis is traditionally perceived as an STD, we could show that using a CD model without refined population structure to address the outbreak of the disease can lead to a good estimate of the epidemic size in a well-mixed gender population. Our CD model can be useful in situations where little in

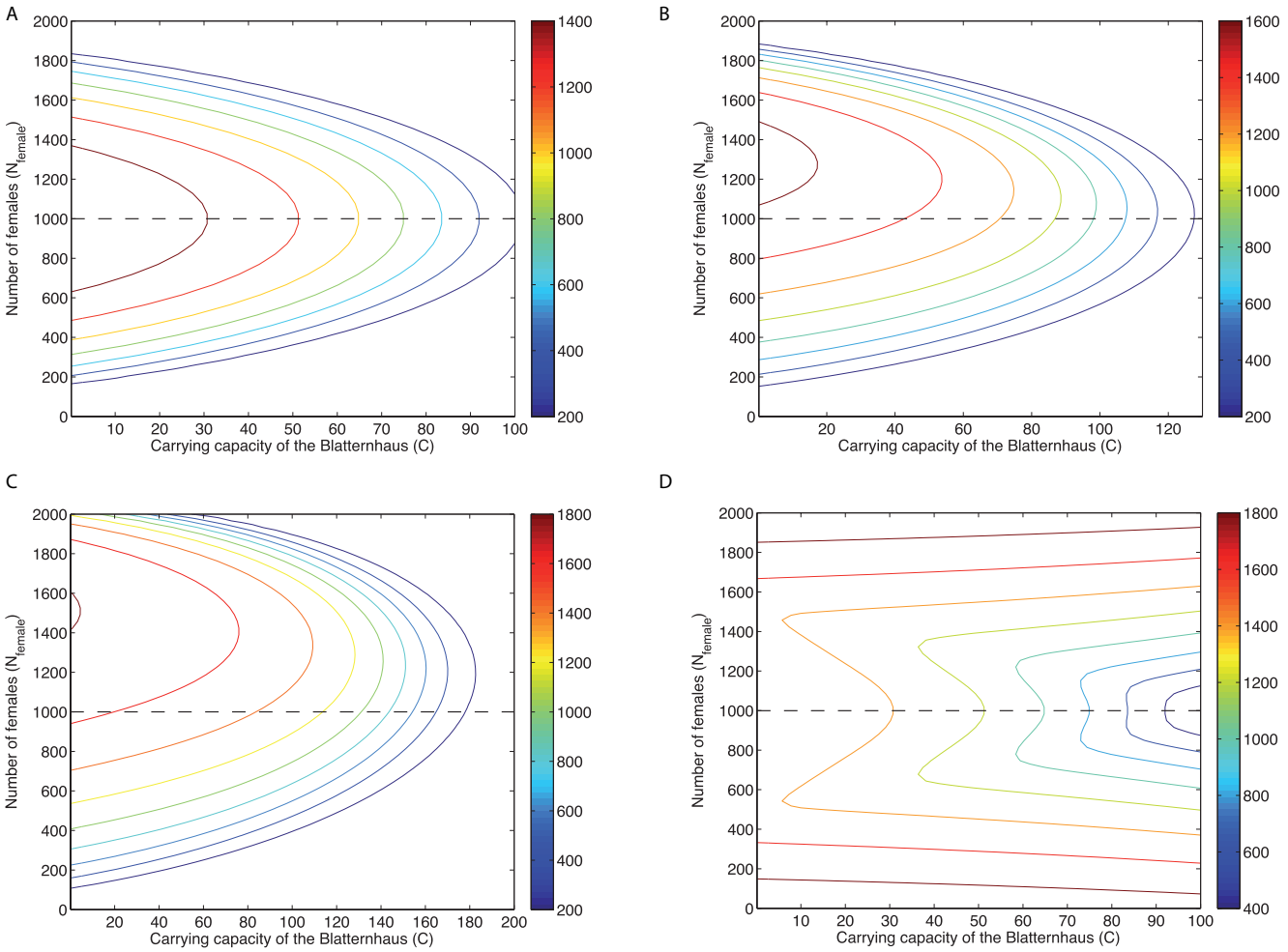

Figure 8: Contour maps of R_{max} isolines for the STD model with no false detection. In (A) all the rates between males and females are equal, and there is no MSM and FSF. In (B) the force of infection for males is larger than for females, and there is no MSM and FSF. In (C) the force of infection for males is larger than for females, and we added MSM and FSF. (D) illustrates the situation where only MSM and FSF are present. The parameters of the plot can be obtained from Figure 2, excepted for (B) where $k_1^{\male} = 5/6(k_1^{\male} + k_1^{\female})$ and $k_1^{\female} = 1/6(k_1^{\male} + k_1^{\female})$, (C) where $k_1^{\male\male} = 5/6(k_1^{\male\male} + k_1^{\female\female})$, and $k_1^{\female\female} = 1/6(k_1^{\male\male} + k_1^{\female\female})$, and (D) where $k_1^{\male\male} = k_1^{\female\female} = 2.2 \cdot 10^{-5}$. The contours are determined by systematically varying the number of females, and keeping the sum of males and females constant.

known about the population habits, or when infectious contact diseases such as leprosy for instance are still prevailing.

The choice of using an STD model instead of a CD model is mainly determined by the type of disease and the knowledge we have about its transmission. In the case of an STD model, the epidemic size is smaller compared to the results obtained with a CD model, because we often assume that sexually active individuals constitute only a subset of the population. Our analysis in section 2 and 3 tends to show that, unless the rates for males and females are different, an STD model will not bring more accurate predictions on the epidemic size. This is particularly true in societies with well mixed-gender behavior composed of heterosexual and homosexual individuals. STD models are relevant in situations where males and females are unevenly distributed, or they respond differently to the disease. The former is more likely to happen in small colonies, or after a major event like a war or a natural disaster. The latter can occur if the force of infection differs between the sexes or for different classes of sexual encounter.

Realistic models of STDs are difficult to establish for many reasons. First, STDs are dependent on social behaviors which have to be documented by empirical observations of social patterns. Second, it is not necessarily the case that these patterns can be easily expressed in tractable mathematics. Refined models based on typical social patterns such as partnership formation and dissolution [22, 23], sexual network formations [24], or concurrent partnership [25] have been analyzed by various authors (see also [26, 27, 28]), and more recently in the context of HIV/AIDS transmission [29, 30]. However such models are susceptible to unreliable data since sexual intercourses are difficult to track through statistical surveys or marital status. Without having the level of sophistication of these models, our model offers the benefit of relying on few parameters, beside the usual rates present in all SIR systems.

Syphilis has many clinical manifestations that make it sometimes difficult to differentiate from other diseases, for instance *pityriasis rosea*: a skin rash that appears similar to secondary syphilis [31]. Syphilis is called by physicians the *chameleon*

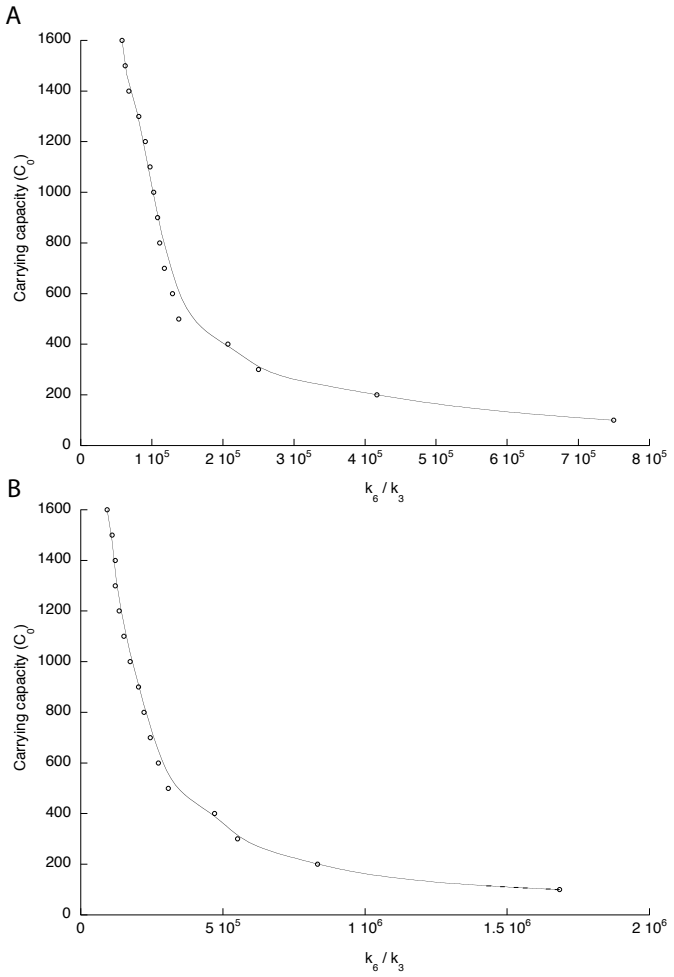

Figure 9: Ratio of true to false detections in the CD (A) and STD (B) models in relation to C_0, which is the carrying capacity at which R_{max} is at most less than 0.1% of the total population. The data points were fitted by using a Stineman smoothing function of all data in *KaleidaGraph*. The parameters of the runs can be obtained from Figure 2 and 4.

of diseases, due to its variety of presentations. For this reason, even nowadays, individuals infected with syphilis for the first time may not notice it themselves. As a consequence, primary and secondary syphilis may remain uncured until the disease enters into a chronic stage where it becomes latent, and symptoms can reappear several years after. Because of these aspects, and others not mentioned here, the disease can easily become endemic. In that case, our model would require further improvements. For instance by incorporating birth and death rates.

5. Conclusion

When encountering an emerging infectious disease for which there is no effective cure, societies have often resorted to implementing a quarantine strategy. Using a theoretical model and 16th century Zurich as a case study, we show that quarantine can be an effective strategy in preventing or reducing an epidemic. As the carrying capacity of the quarantine facility increases, control of the epidemic becomes easier. In our case study with a city of 4000 individuals, we see that a carrying capacity on the order of 100 individuals can stop most epidemics with $R_0 \leq 2$. However, we also see that this strategy requires a detection procedure that selects mainly infected individuals, and minimizes false detections. Hence indiscriminate quarantine measures can be counterproductive. The root of this phenomenon is explained by the carrying capacity of the quarantine facility and the space taken by non infectious individuals. By filling up the quarantine facility, false detections prevent infected individuals from being quarantined. Therefore, improving true detection and avoiding false positives becomes the key factor in implementing successful quarantines.

In the case of sexually transmitted diseases, additional factors that influence the effectiveness of control are asymmetries in the ratio of males to females, differences in the sexes pertaining to the force of infection, and differences in transmission rates due to different forms of partner pairings. Generally, when the force of infection is the same for both male and female partners, moving away from a 1:1 male to female ratio can ease the control of the epidemic. However, when males and females are subject to asymmetric forces of infection, then asymmetries in the male to female ratios can lead to unexpected difficulties. For example, a heterosexually transmitted disease that mainly affects males is harder to control in a population with more females (and *vice versa*). Hence situations that lead to an unbalance in the sex ratios (such as mining colonies or populations at war) can lead to the failure of quarantine efforts.

6. Acknowledgment

The work was supported in part by NSF grant 31003A-125457, the Kanton Zurich and the RPH-Promotor Stiftung. We are grateful to Valentina Rossetti, Manuela Filippini, and Bettina Schirrmeister for their comments on the manuscript, and to Dr. Annelies Zinkernagel for her valuable highlights on the clinical aspects of syphilis.

References

[1] E. W. Hook, R. W. Peeling, Syphilis control – a continuing challenge, N Engl J Med 351 (2) (2004) 122–4.
[2] M. Hvistendahl, An explosive return of the 'great pox', Science 335 (2012) 390.
[3] Syphilis in deutschland im jahr 2009, das Robert Koch Institut (2010).
[4] G. E. Gall, S. Lautenschlager, H. C. Bagheri, Public health response of the city of zurich to epidemic syphilis at the dawn of the modern era (1496-1585), preprint (2012).
[5] T. Day, A. Park, N. Madras, A. Gumel, J. Wu, When is quarantine a useful control strategy for emerging infectious diseases?, Am J Epidemiol 163 (5) (2006) 479–485.
[6] Z. Feng, H. R. Thieme, Recurrent outbreaks of childhood diseases revisited: the impact of isolation, Math Biosci 128 (1-2) (1995) 93–130.
[7] H. Hethcote, M. Zhien, L. Shengbing, Effects of quarantine in six endemic models for infectious diseases, Math Biosci 180 (2002) 141–160.
[8] J. M. Hyman, J. Li, Modeling the effectiveness of isolation strategies in preventing std epidemics, Siam Journal on Applied Mathematics 58 (3) (1998) 912–925.
[9] L. Sattenspiel, D. A. Herring, Simulating the effect of quarantine on the spread of the 1918-19 flu in central canada, Bull Math Biol 65 (1) (2003) 1–26.

[10] C. Fraser, S. Riley, R. M. Anderson, N. M. Ferguson, Factors that make an infectious disease outbreak controllable, Proceedings of the National Academy of Sciences of the United States of America 101 (16) (2004) 6146–6151.
[11] W. O. Kermack, A. G. McKendrick, A contribution to the mathematical theory of epidemics, Proceedings of the Royal Society of London. Series A 115 (772) (1927) 700–721.
[12] J. D. Murray, Mathematical Biology. I. An Introduction, Vol. 17 of Interdisciplinary Applied Mathematics, Springer, Berlin and Heidelberg, 1993.
[13] O. Diekmann, J. A. Heesterbeek, J. A. Metz, On the definition and the computation of the basic reproduction ratio r0 in models for infectious diseases in heterogeneous populations, J Math Biol 28 (4) (1990) 365–82.
[14] J. M. Hyman, J. Li, An intuitive formulation for the reproductive number for the spread of diseases in heterogeneous populations, Math Biosci 167 (1) (2000) 65–86.
[15] M. J. Keeling, P. Rohani, Modeling Infectious Diseases in humans and animals, Princeton University Press, Princeton and Oxford, 2008.
[16] R. M. Anderson, R. M. May, Population biology of infectious diseases: Part 1, Nature 280 (5721) (1979) 361–7.
[17] H. W. Hethcote, The mathematics of infectious diseases, SIAM 42 (1) (2000) 599–653.
[18] http://www.cdc.gov/std/syphilis/stdfact-syphilis.htm.
[19] http://www.merckmanuals.com/professional/index.html.
[20] A. S. Evans, P. S. Brachman, Bacterial Infections of Humans: Epidemiology and Control, Kluwer academic, New York, 1998.
[21] G. P. Garnett, An introduction to mathematical models in sexually transmitted disease epidemiology, Sex Transm Infect 78 (1) (2002) 7–12.
[22] S. J. Nelson, J. P. Hughes, B. Foxman, S. O. Aral, K. K. Holmes, P. J. White, M. R. Golden, Age- and gender-specific estimates of partnership formation and dissolution rates in the seattle sex survey, Annals of Epidemiology 20 (4) (2010) 308–17.
[23] M. Artzrouni, E. Deuchert, Consistent partnership formation: application to a sexually transmitted disease model, Mathematical Biosciences 235 (2) (2012) 182–8.
[24] A. C. Ghani, J. Swinton, G. P. Garnett, The role of sexual partnership networks in the epidemiology of gonorrhea, Sex Transm Dis 24 (1) (1997) 45–56.
[25] N. M. Ferguson, G. P. Garnett, More realistic models of sexually transmitted disease transmission dynamics, Sex Transm Dis 27 (10) (2000) 600–609.
[26] R. M. Anderson, G. P. Garnett, Mathematical models of the transmission and control of sexually transmitted diseases, Sex Transm Dis 27 (10) (2000) 639–643.
[27] K. T. D. Eames, M. J. Keeling, Modeling dynamic and network heterogeneities in the spread of sexually transmitted diseases, Proc Natl Acad Sci USA 99 (20) (2002) 13330–5.
[28] C. Castillo-Chavez, H. Hethcote, V. Andreasen, S. Levin, W. M. Liu, Epidemiological models with age structure, proportionate mixing, and cross-immunity, Journal of Mathematical Biology 27 (3) (1989) 233–258.
[29] O. M. Akpa, B. A. Oyejola, Modeling the transmission dynamics of hiv/aids epidemics: an introduction and a review, J Infect Dev Ctries 4 (10) (2010) 597–608.
[30] J. M. Hyman, J. Li, E. A. Stanley, Threshold conditions for the spread of the hiv infection in age-structured populations of homosexual men, J Theor Biol 166 (1) (1994) 9–31.
[31] T. Horn, A. Kazakis, Pityriasis rosea and the need for a serologic test for syphilis, Cutis 39 (1) (1987) 81–82.

Renaissance model of an epidemic with quarantine

Akos Dobay[1], Gabriella E. C. Gall [1], Daniel J. Rankin[1], Homayoun C. Bagheri [1]

[1]Institute of Evolutionary Biology and Environmental Studies, Winterthurerstrasse 190, University of Zurich, CH-8057 Zurich, Switzerland

1. The relative removal rate ρ and the basic reproduction rate R_0

We are interested to derive an expression for ρ and R_0 in our model. In both cases, we start with the following general assumption

$$S(0) = S_0 > 0, I(0) = I_0 > 0, R(0) = 0,$$

and

$$S_B(0) = S_{B,0} > 0, I_B(0) = I_{B,0} > 0.$$

We first derive an expression for ρ by solving $\frac{dI}{dt}$ for $t = 0$, that is

$$\frac{dI}{dt}|_{t=0} = I_0\,(k_1 S_0 - k_2 - \kappa_{CD} k_6) + k_7 I_{B,0}, \quad \begin{cases} > 0 \\ < 0 \end{cases} \quad \text{if} \quad S_0 \begin{cases} > \rho(C) \\ < \rho(C), \end{cases}$$

and where

$$\rho(C) = \frac{k_2 I_0 + k_6(C - S_{B,0} - I_{B,0}) I_0 - k_7 I_{B,0}}{k_1 I_0}. \tag{1}$$

As we can notice, the relative removal rate is dependent on the carrying capacity C, the number of susceptible S_B and infected I_B individual in the *Blatternhaus*.

An expression for basic reproduction rate R_0 can be obtained by starting from our previous result summarized in 1 for the relative removal rate. Given a force of infection k_1 per capita, the rate at which individuals are effectively removed from the population is proportional to $k_2 + k_6(C - S_{B,0} - I_{B,0}) - k_7$. Therefore, the basic reproduction rate R_0 for the whole population becomes

$$R_0 = \frac{k_1 S_0}{k_2 + k_6(C - S_{B,0} - I_{B,0}) - k_7}. \tag{2}$$

2. The equilibrium analysis using the standard Jacobian approach

In this section, we looked at the equilibrium analysis for the contact disease model. The equilibrium analysis will address the question whether the steady state is stable or not, and whether it is dependent on the rates defined in the model. The steady state is given by

$$\begin{aligned} -k_1 S I - \kappa_{CD} k_3 S + k_4 S_B &= 0 \\ -k_5 S_B I_B + \kappa_{CD} k_3 S - k_4 S_B &= 0 \\ k_1 S I - k_2 I - \kappa_{CD} k_6 I + k_7 I_B &= 0 \\ \kappa_{CD} k_6 I - k_7 I_B + k_5 S_B I_B - k_8 I_B &= 0 \\ k_2 I + k_8 I_B &= 0 \end{aligned}$$

For simplicity we assume that $S_B(0) = 0$ and $I_B(0) = 0$, which reduces κ_{CD} to C. Then, using numerical routines in *Mathematica*, we find three set of equilibrium points. The first set of points

$$(\bar{S}, \bar{S}_B, \bar{I}, \bar{I}_B, \bar{R}) = (\bar{S}, \frac{k_3 C \bar{S}}{k_4 + k_3 \bar{S}}, 0, 0, \bar{R}) \tag{3}$$

depends on k_3, k_4 and C. It corresponds to the situation where susceptible individuals are sent to quarantine and released at a given frequency k_3 and k_4 without getting infected. In the case where k_3 is zero, the equilibrium points describe a population of susceptible individuals S that neither get infected, nor sent to quarantine. The population of susceptible individuals S stays constant over time, and it is equal to N. This solution reduces to the disease free equilibrium

$$(\bar{S}, \bar{S}_B, \bar{I}, \bar{I}_B, \bar{R}) = (N, 0, 0, 0, \bar{R}).$$

It is noteworthy to observe that this solution involves the carrying capacity C of the facility. It corresponds to the situation where the quarantine facility is used without having a real epidemic that would justify its usage.

The second set of points

$$\begin{cases} S = 0 \\ S_B = 0 \\ I = -\dfrac{Ck_6k_8 + k_2(k_7 + k_8)}{k_6k_8} \\ I_B = \dfrac{Ck_6k_8 + k_2(k_7 + k_8)}{k_6k_8} \end{cases}$$

involves the rates k_2, k_6, k_7 and k_8, which are specific to the infected compartments I and I_B. This steady state has a physical meaning only if $I = I_B = 0$, which implies that

$$Ck_6k_8 + k_2(k_7 + k_8) = 0.$$

This condition can be only achieved if $k_2 = 0$, together with $k_6 = 0$ or $k_8 = 0$. In other words, the second set of equilibrium points is equivalent to the trivial solution

$$(\bar{S}, \bar{S}_B, \bar{I}, \bar{I}_B, \bar{R}) = (0, 0, 0, 0, \bar{R}). \tag{4}$$

The third set of points

$$\begin{cases} S = \dfrac{k_2\left(k_1k_6k_8^2(k_4 + Ck_5) + k_2^2k_3k_5(k_7 + k_8) + k_1k_2k_5k_8(k_7 + k_8)\right)}{k_1k_8(k_2^2k_3k_5 + k_1k_2k_5k_8 + k_1k_6k_8^2)} \\ S_B = \dfrac{k_1k_6k_8^2(k_4 + Ck_5) + k_2^2k_3k_5(k_7 + k_8) + k_1k_2k_5k_8(k_7 + k_8)}{k_5(k_2^2k_3k_5 + k_1k_2k_5k_8 + k_1k_6k_8^2)} \\ I = \dfrac{k_8\left(-Ck_2^2k_3k_5^2 + k_1k_2k_4k_5k_8 + k_1k_4k_6k_8^2 + k_2^2k_3k_5(k_7 + k_8)\right)}{k_2k_5(k_2^2k_3k_5 + k_1k_2k_5k_8 + k_1k_6k_8^2)} \\ I_B = -\dfrac{-Ck_2^2k_3k_5^2 + k_1k_2k_4k_5k_8 + k_1k_4k_6k_8^2 + k_2^2k_3k_5(k_7 + k_8)}{k_5(k_2^2k_3k_5 + k_1k_2k_5k_8 + k_1k_6k_8^2)} \end{cases} \tag{5}$$

requires that

$$-Ck_2^2k_3k_5^2 + k_1k_2k_4k_5k_8 + k_1k_4k_6k_8^2 + k_2^2k_3k_5(k_7 + k_8) = 0.$$

In this case, the set of equilibrium points describe again a situation with no infected individuals, and where susceptible individuals are sent to quarantine and release at a given frequency.

Using the solutions we found previously, we can now compute the Jacobian to analyze whether the three set of equilibrium points are stable or not. First, we define the set of functions associated to the model using the following

convention

$$\begin{cases} \frac{dS}{dt} = f_1(S, I, R, S_B, I_B) = -k_1 S I - \kappa_{STD} k_3 S + k_4 S_B \\ \frac{dS_B}{dt} = f_2(S, I, R, S_B, I_B) = -k_5 S_B I_B + \kappa_{STD} k_3 S - k_4 S_B \\ \frac{dI}{dt} = f_3(S, I, R, S_B, I_B) = k_1 S I - k_2 I - \kappa_{STD} k_6 I + k_7 I_B \\ \frac{dI_B}{dt} = f_4(S, I, R, S_B, I_B) = \kappa_{STD} k_6 I - k_7 I_B + k_5 S_B I_B - k_8 I_B \\ \frac{dR}{dt} = f_5(S, I, R, S_B, I_B) = k_2 I + k_8 I_B \end{cases}.$$

From this set of functions, we introduce a Jacobian defined as

$$J = \begin{pmatrix} \frac{\partial f_1}{\partial S} & \frac{\partial f_1}{\partial I} & \frac{\partial f_1}{\partial R} & \frac{\partial f_1}{\partial S_B} & \frac{\partial f_1}{\partial I_B} \\ \frac{\partial f_2}{\partial S} & \frac{\partial f_2}{\partial I} & \frac{\partial f_2}{\partial R} & \frac{\partial f_2}{\partial S_B} & \frac{\partial f_2}{\partial I_B} \\ \frac{\partial f_3}{\partial S} & \frac{\partial f_3}{\partial I} & \frac{\partial f_3}{\partial R} & \frac{\partial f_3}{\partial S_B} & \frac{\partial f_3}{\partial I_B} \\ \frac{\partial f_4}{\partial S} & \frac{\partial f_4}{\partial I} & \frac{\partial f_4}{\partial R} & \frac{\partial f_4}{\partial S_B} & \frac{\partial f_4}{\partial I_B} \\ \frac{\partial f_5}{\partial S} & \frac{\partial f_5}{\partial I} & \frac{\partial f_5}{\partial R} & \frac{\partial f_5}{\partial S_B} & \frac{\partial f_5}{\partial I_B} \end{pmatrix}.$$

After making the appropriate derivation in the Jacobian, we obtain the following matrix

$$J = \begin{pmatrix} k_3(S_B - C + I_B) - k_1 I & -k_1 S & 0 & k_3 S + k_4 & k_3 S \\ k_3(C - S_B - I_B) & 0 & 0 & -k_3 S - k_4 - k_5 I_B & -k_3 S - k_5 S_B \\ k_1 I & k_1 S - k_2 + k_6(S_B - C + I_B) & 0 & k_6 I & k_6 I + k_7 \\ 0 & k_6(C - S_B - I_B) & 0 & k_5 I_B - k_6 I & -k_6 I + k_5 S_B - k_7 - k_8 \\ 0 & k_2 & 0 & 0 & k_8 \end{pmatrix}. \quad (6)$$

Then, by replacing the first set of points $(N, \frac{k_3 CN}{k_4 + k_3 N}, 0, 0, \bar{R})$ in the Jacobian we get

$$\begin{pmatrix} \frac{k_3^2 k_4 C}{k_4 + k_3 N} - k_3 C & -k_1 N & 0 & k_3 N + k_4 & k_3 N \\ \frac{-k_3^2 k_4 C}{k_4 + k_3 N} + k_3 C & 0 & 0 & -k_3 N - k_4 & \frac{-k_3 k_5 CN}{k_4 + k_3 N} - k_3 N \\ 0 & k_1 N - k_2 - \frac{k_4 k_6 C}{k_4 + k_3 N} & 0 & 0 & k_7 \\ 0 & \frac{k_4 k_6 C}{k_4 + k_3 N} & 0 & 0 & \frac{k_3 k_5 CN}{k_4 + k_3 N} - k_7 - k_8 \\ 0 & k_2 & 0 & 0 & k_8 \end{pmatrix}. \quad (7)$$

To further simplify the eigenvalues, we decided to replace the actual values of the rates used for the numerical analysis directly in our matrix. For both cases, $k_3 = 0$ and $k_3 = 2 \cdot 10^{-7}$, and for C ranging from 0 to 100, we obtain one positive eigenvalue. Hence, the first set of equilibrium points is unstable.

The second set of equilibrium points $(\bar{S}, \bar{S}_B, \bar{I}, \bar{I}_B, \bar{R}) = (0, 0, 0, 0, \bar{R})$ gives

$$\begin{pmatrix} -k_3 C & 0 & 0 & k_4 & 0 \\ k_3 C & 0 & 0 & -k_4 & 0 \\ 0 & -k_2 - k_6 C & 0 & 0 & k_7 \\ 0 & k_6 C & 0 & 0 & -k_8 - k_7 \\ 0 & k_2 & 0 & 0 & k_8 \end{pmatrix}.$$

After replacing the corresponding rates with their actual values, we found the same type of result as for the first set of equilibrium points: the second set of equilibrium points is also unstable. A similar calculation shows that the third set of equilibrium points is unstable as well.

3. Contact disease model using constant effective quarantine rates

This section provides a variant of our contact disease (CD) model where the effective quarantine rates $\kappa_{CD} k_3$ and $\kappa_{CD} k_6$ are kept constant, and individuals are quarantined as long as there is spare room inside the quarantine facility. This variant is identical in its mathematical form to our CD model presented in the article, except for κ_{CD}, which is defined using the following Heaviside step function

$$\kappa_{CD} = \mathcal{H}(C - S_B - I_B) = \begin{cases} 0 & \text{if} \quad C - S_B - I_B < 0 \\ 1/2 & \text{if} \quad C - S_B - I_B = 0 \\ 1 & \text{if} \quad C - S_B - I_B > 0 \end{cases}.$$

Using numerical routines in *Matlab*, we analyzed the present CD model in the simplest case with no false positives ($k_3 = 0$ and $S_B = 0$). Figure 1A plots the maximum of the total number of infected individuals ($I + I_B$), while Figure 1B displays the total number of removed individuals R, both against the force of infection and the carrying capacity. Depending on the force of infection k_1, the recovery rate k_2 and the quarantine rate k_6, the system reaches an equilibrium point where additional amounts of spare room in the quarantine facility no longer prevent further reductions in the epidemic size.

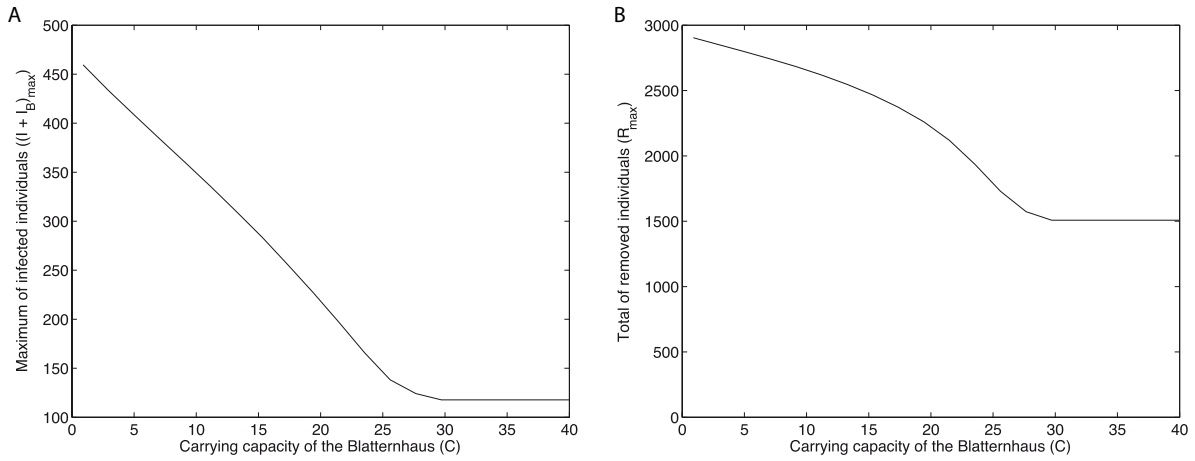

Figure 1: Numerical analysis of the CD model with constant effective quarantine rate $\kappa_{CD} k_6$ and no false detection ($k_3 = 0$ and $S_B = 0$). The profile for the reproduction rate $R_{0,C=0} = 2$ is displayed, showing the relationship between $(I + I_B)_{max}$ (A) and R_{max} (B) and the carrying capacity of the *Blatternhaus*. The remaining parameters in the model, as well as the initial conditions, can be obtained from the article (see for instance Figure 2), excepted k_6 and k_7, which are equal to $5 \cdot 10^{-3}$ and $5 \cdot 10^{-4}$ respectively.

4. Reduction of the sexually transmitted disease model to the contact disease model

This section shows under which circumstances the sexually transmitted disease (STD) model can be rewritten as a contact disease (CD) model. To this aim we use the first two equations of the STD model, defining the state of susceptible individuals, and combine them into one equation. What we obtain is

$$\frac{dS_{\female}}{dt}+\frac{dS_{\male}}{dt} = \left(-k_1^{\female} S_{\female} I_{\male} - k_1^{\female\female} S_{\female} I_{\female} - \kappa_{STD} k_3^{\female} S_{\female} + k_4^{\female} S_{\female B}\right)^{\female} + \left(-k_1^{\male} S_{\male} I_{\female} - k_1^{\male\male} S_{\male} I_{\male} - \kappa_{STD} k_3^{\male} S_{\male} + k_4^{\male} S_{\male B}\right)^{\male}. \tag{8}$$

In the special case where the rates for males and females are equal we can write

$$\begin{cases} \kappa_{STD} = \kappa_{CD} \\ k_3^{\female} = k_3^{\male} = k_3 \\ k_4^{\female} = k_4^{\male} = k_4 \\ k_1^{\female} = k_1^{\male} = k_1 \\ k_1^{\female\female} = k_1^{\male\male} = k_1. \end{cases}$$

By substituting these equalities in 8, we have

$$\begin{aligned} \frac{dS_{\female}}{dt} + \frac{dS_{\male}}{dt} &= \left(-k_1 S_{\female} I_{\male} - k_1 S_{\female} I_{\female} - \kappa_{CD} k_3 S_{\female} + k_4 S_{\female B}\right)^{\female} + \left(-k_1 S_{\male} I_{\female} - k_1 S_{\male} I_{\male} - \kappa_{CD} k_3 S_{\male} + k_4 S_{\male B}\right)^{\male} \\ &= -k_1 (S_{\female} I_{\male} + S_{\female} I_{\female} + S_{\male} I_{\female} + S_{\male} I_{\male}) - \kappa_{CD} k_3 (S_{\female} + S_{\male}) + k_4 (S_{\female B} + S_{\male B}) \\ \frac{d(S_{\female} + S_{\male})}{dt} &= -k_1 (S_{\female} + S_{\male})(I_{\female} + I_{\male}) - \kappa_{CD} k_3 (S_{\female} + S_{\male}) + k_4 (S_{\female B} + S_{\male B}). \end{aligned}$$

We can further write that

$$\begin{cases} S = S_{\male} + S_{\female} \\ I = I_{\male} + I_{\female} \\ S_B = S_{\male B} + S_{\female B}, \end{cases}$$

which reduces 8 to

$$\frac{dS}{dt} = -k_1 S I - \kappa_{CD} k_3 S + k_4 S_B.$$

5. Supplementary figures

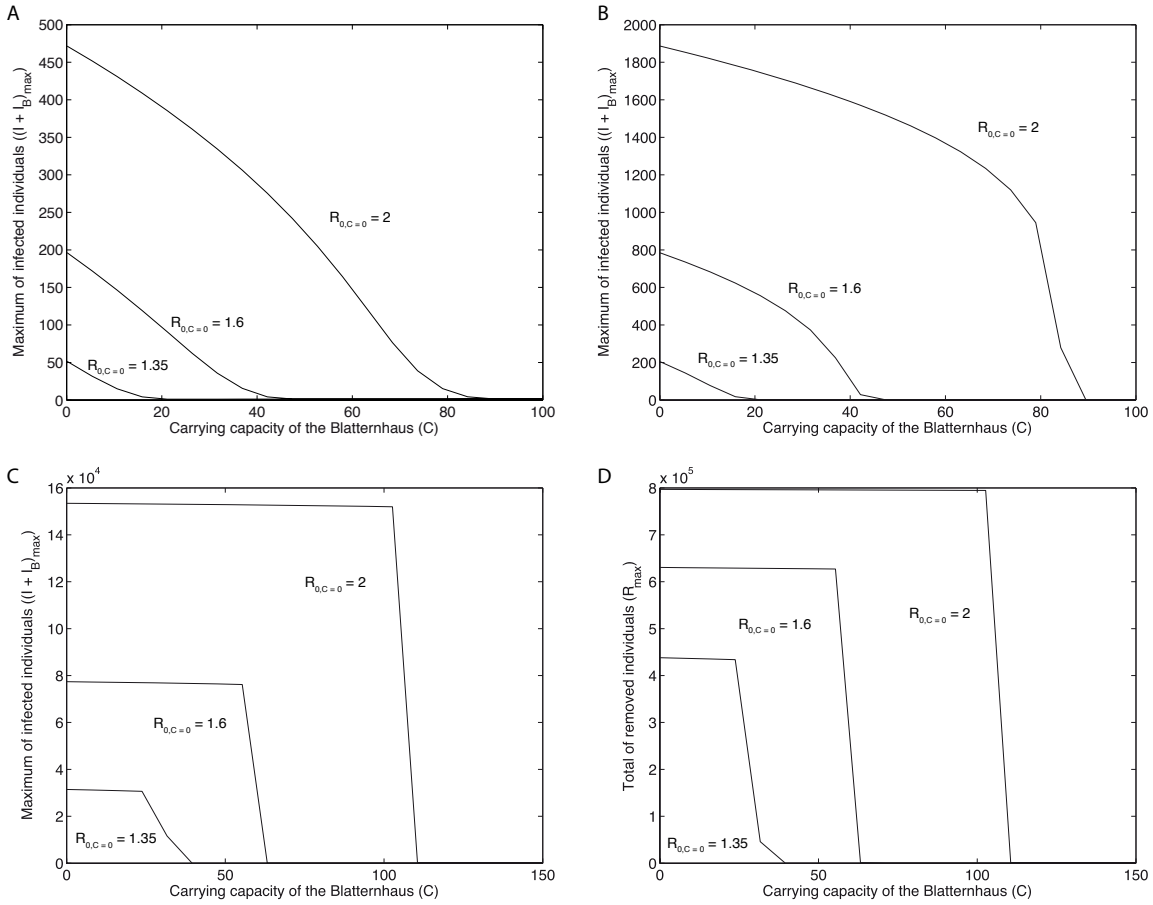

Figure 2: Numerical analysis of the CD model with no false detection ($S_B = 0$ and $k_3 = 0$). The maximum of the total number of infected individuals inside and outside the *Blatternhaus* $(I + I_B)_{max}$ is compared for two different population sizes: (A) $N = 4'000$. (B) $N = 16'000$. (C and D) $N = 10^6$. The remaining parameters can be obtained from Figure 2 in the article.

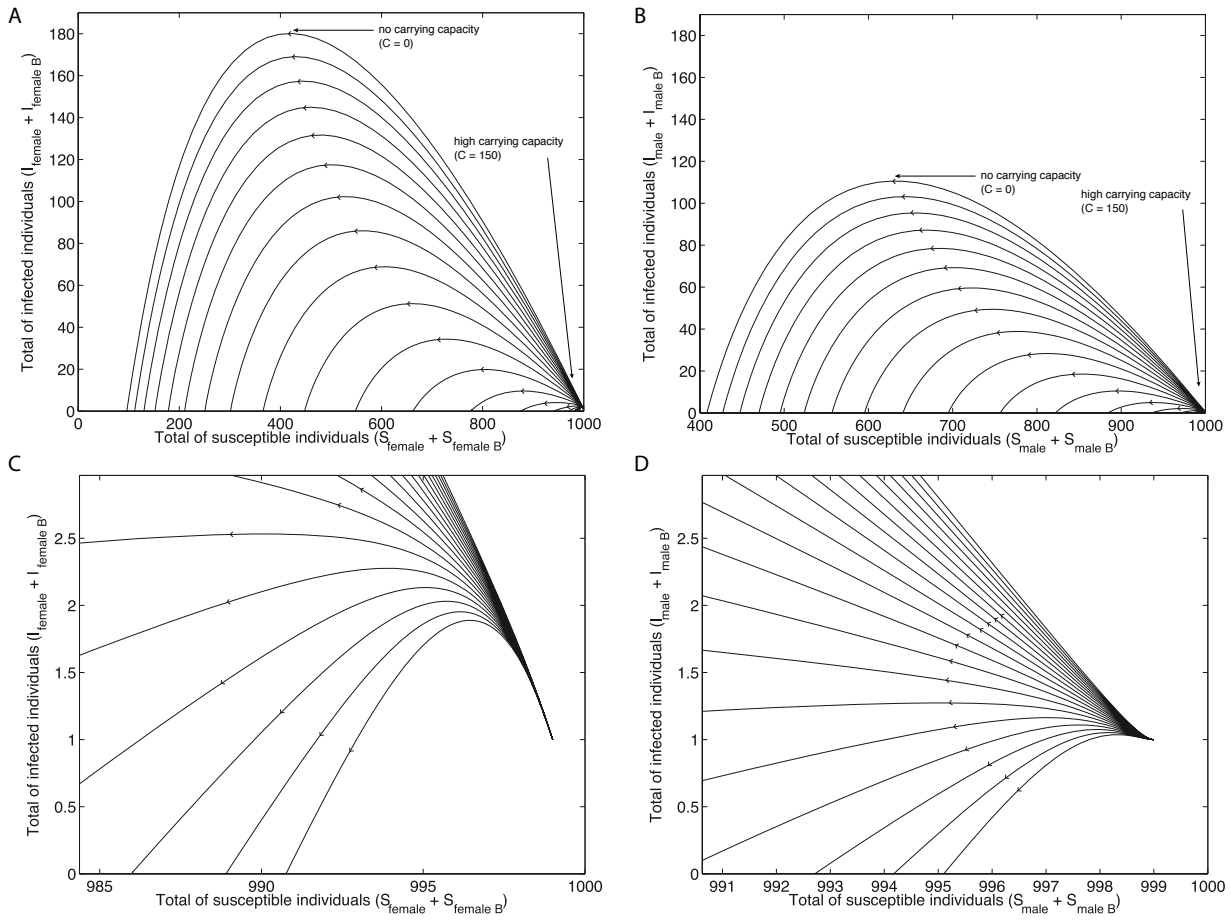

Figure 3: Numerical analysis of the STD model with no false detection and with a larger force of infection for females ($k_1^{\female} = 4 \cdot k_1^{\male}$). For this analysis, we increased the carrying capacity to 150. (A to D) Phase trajectories in the susceptible versus total infected individuals plane. (C and D) A detailed view of the model behavior at large carrying capacities shows how the discrepancy in the force of infection can be compensated by the size of the quarantine facility. The other parameters in the model are the population size $N = 2'000$, $k_1^{\male} = 1 \cdot 10^{-5}$, $k_2 = 1/90$, $k_4^{\male} = k_4^{\female} = k_5^{\male} = k_5^{\female} = 0$, $k_6^{\male} = k_6^{\female} = 1 \cdot 10^{-4}$, $k_7^{\male} = k_7^{\female} = 1 \cdot 10^{-5}$, $k_8 = 1/70$, $k_1^{\male\male} = k_5^{\male\male} = k_1^{\female\female} = k_5^{\male\male} = 0$. The trajectories are determined by the initial conditions $S_{\male}(0) = 999$, $S_{\female}(0) = 999$, $S_{\male B}(0) = 0$, $S_{\female B}(0) = 0$, $I_{\male}(0) = 1$, $I_{\female}(0) = 1$, $I_{\male B}(0) = 0$, $I_{\female B}(0) = 0$ and $R(0) = 0$.

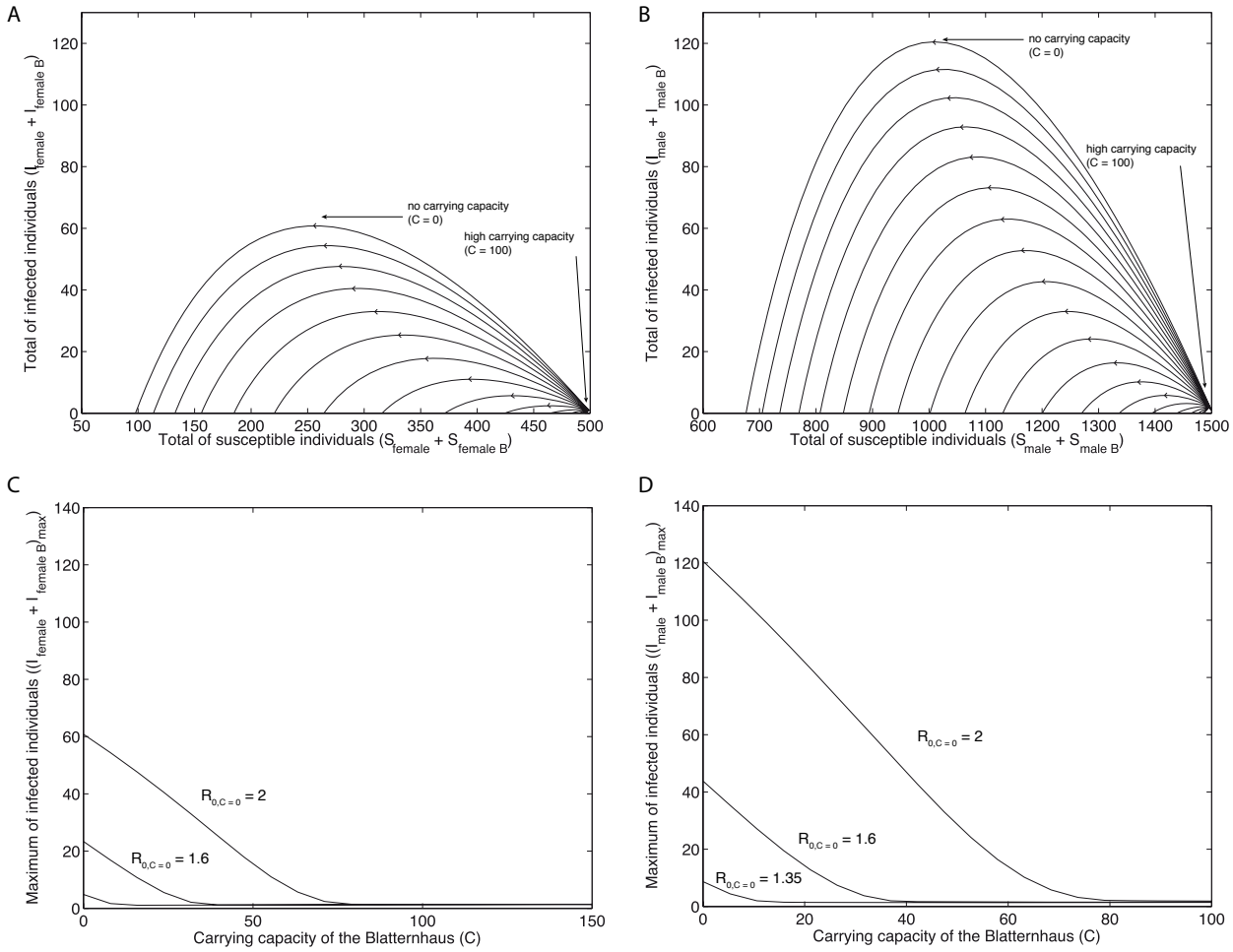

Figure 4: Numerical analysis of the STD model with no false detection ($S_B = 0$ and $k_3 = 0$) and with an asymmetric number of males (500) and females (1'500). (A and B) Phase trajectories in the susceptible versus total infected individuals plane. (C and D) Maximum of infected individuals versus the carrying capacity of the *Blatternhaus*. The parameters in the model can be obtained from Figure 2. The initial conditions are $S_{♂}(0) = 499$, $S_{♀}(0) = 1'499$, $S_{♂B}(0) = 0$, $S_{♀B}(0) = 0$, $I_{♂}(0) = 1$, $I_{♀}(0) = 1$, $I_{♂B}(0) = 0$, $I_{♀B}(0) = 0$ and $R(0) = 0$.

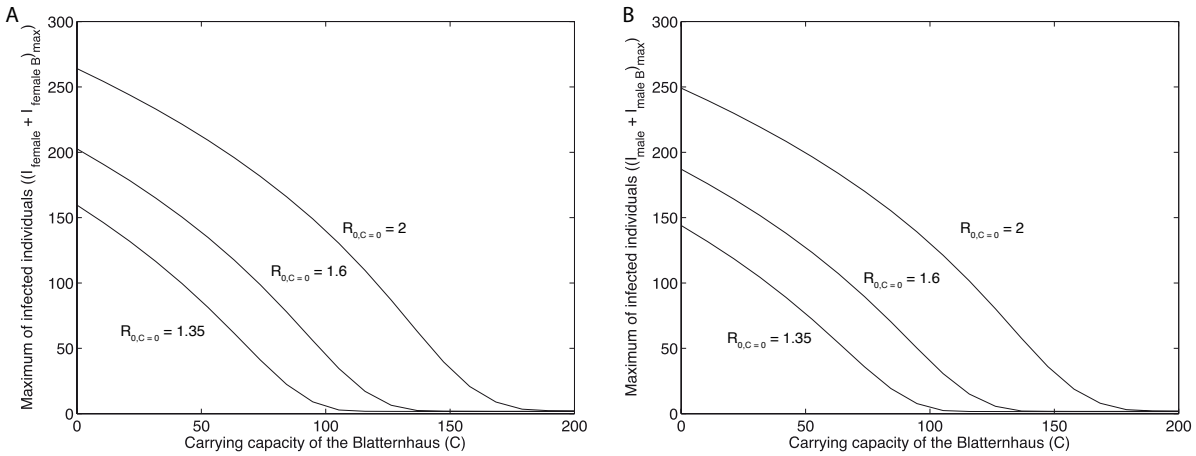

Figure 5: Numerical analysis of the STD model with no false detection and homosexual intercourses. The parameters in the model are the population size $N = 2'000$, $k_2 = 1/90$, $k_4^{\male} = k_4^{\female} = k_5^{\male} = k_5^{\female} = 0$, $k_6^{\male} = k_6^{\female} = 1 \cdot 10^{-4}$, $k_7^{\male} = k_7^{\female} = 1 \cdot 10^{-5}$, $k_8 = 1/70$, $k_1^{\male\male} = 5 \cdot 10^{-6}$, $k_5^{\male\male} = 0$, and $k_1^{\female\female} = 1 \cdot 10^{-5}$, $k_5^{\female\female} = 0$. The initial conditions are $S_{\male}(0) = 999$, $S_{\female}(0) = 999$, $S_{\male B}(0) = 0$, $S_{\female B}(0) = 0$, $I_{\male}(0) = 1$, $I_{\female}(0) = 1$, $I_{\male B}(0) = 0$, $I_{\female B}(0) = 0$ and $R(0) = 0$.

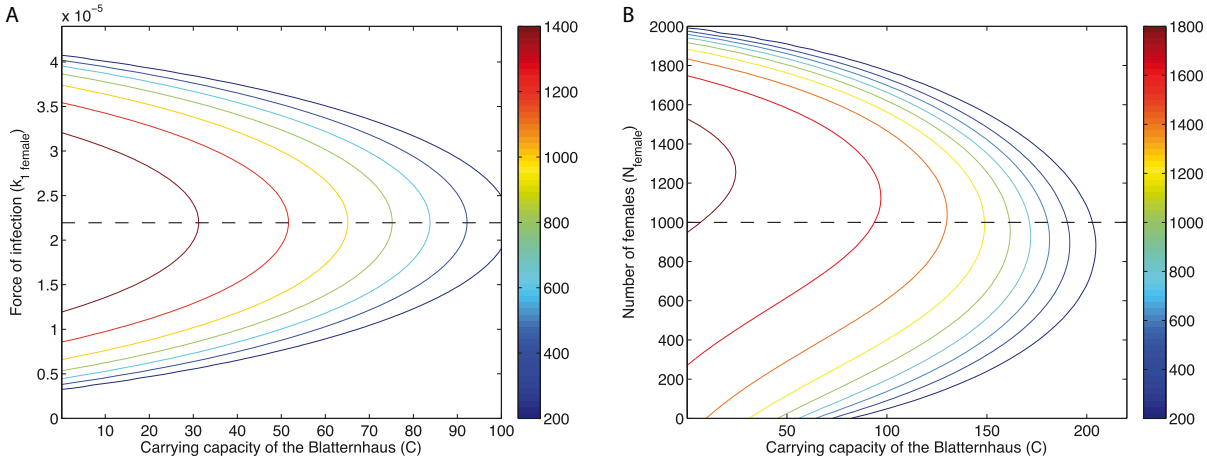

Figure 6: Contour maps of R_{max} isolines of the STD model with no false detection. In (A) the number of males and females is equal, and there is no MSM and FSF. The contours are determined by systematically varying the force of infection for females, and keeping the sum of the force of infection for males and females constant. In (B) we added MSM and FSF encounters, and we also set the force of infection to be larger for males among heterosexual encounters, and to be larger for females among homosexual encounters. The parameters of the plot can be obtained from Figure 2, excepted for (B) where $k_1^{\male} = 5/6(k_1^{\male} + k_1^{\female})$ and $k_1^{\female} = 1/6(k_1^{\male} + k_1^{\female})$, and $k_1^{\male\male} = 1/6(k_1^{\male\male} + k_1^{\female\female})$ and $k_1^{\female\female} = 5/6(k_1^{\male\male} + k_1^{\female\female})$.

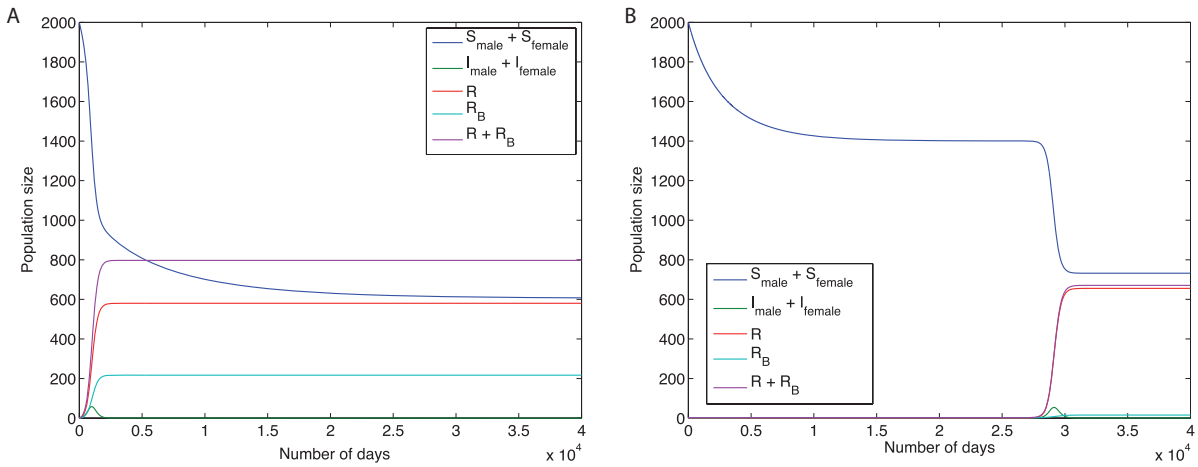

Figure 7: STD model with false detections. For large carrying capacity compare to the population size, the epidemic mostly occurs outside the *Blatternhaus* as a result of false detections. To highlight this point, we divided the recovered individuals in two groups. The red line (R) denotes the recovered individuals outside the *Blatternhaus*, while the cyan line (R_B) indicates the recovered individuals inside the *Blatternhaus*. Susceptible males and females outside the *Blatternhaus* are shown in blue. In both cases, $C = 600$ and in (B) $k_6^{\male} = k_6^{\female} = 1 \cdot 10^{-3}$. The other parameters can be obtained from Figure 2 and 4 in the article.